OPTIMIZED REHABILITATION OF WATER PIPE NETWORKS SUBJECTED TO EARTHQUAKES

by

BINAYA PUDASAINI

DISSERTATION

Submitted in partial fulfillment of the requirements

for the degree of Doctor of Philosophy at

The University of Texas at Arlington

August 2019

Arlington, Texas

Supervising Committee:

Dr. Mohsen Shahandashti, Supervising Professor

Dr. Shih-Ho Chao

Dr. Jay Rosenberger

Dr. Suyun Ham

Disclaimer

Any opinions, findings, and conclusions or recommendations expressed in this material are those of the author(s) and do not necessarily reflect the views of the National Science Foundation.

Acknowledgments

First and foremost, I would like to thank my PhD supervising professor Dr. Mohsen Shahandashti for his constant guidance, supervision, and support. Without his vision, his encouragement, and his faith in me, I would never have been able to complete my PhD. He has been an immensely good mentor to me, and I have been fortunate enough to learn so much from him in these past four years. I am also grateful to Dr. Chao, Dr. Rosenberger, and Dr. Ham for finding time out of their busy schedule to be in my PhD supervising committee and for guiding me in this research through their insightful and incisive comments.

I would also like to convey my gratitude to my lab mates who have always been there to support me through thick and thin. I was really blessed with lab mates who were not only colleagues but true friends and who were a constant source of encouragement and inspiration.

I also want to thank my family for their faith, belief, and unwavering support. Specifically, I want to thank my father for making me dream of having a PhD someday; I want to thank my mother for making me believe that no ambition was too big for me if I worked hard enough; and I want to thank my brother for his belief in me. I also want to thank my wife for her invaluable company, her relentless critique, and her unwavering love. For these last four years, she has been the first voice to rejoice besides me during the good times and the first hand to offer help during some hard times. Without her, this PhD journey would have been a lot harder and significantly less enjoyable.

Abstract

OPTIMIZED REHABILITATION OF WATER PIPE NETWORKS SUBJECTED TO

EARTHQUAKES

Binaya Pudasaini, PhD

The University of Texas at Arlington, 2019

Supervising Professor: Dr. Mohsen Shahandashti

Earthquakes in the past and in the recent times have demonstrated the extreme vulnerability of the water pipe networks. The impacts of such earthquakes on the water supply network can lead to significant direct and indirect losses. These losses highlight the critical need for seismic rehabilitation of water pipe network. Despite such criticality, water supply network managers are often constrained in what they can do with the limited rehabilitation budget that they have access to. Majority of current models dealing with seismic vulnerability assessment of water pipes do not provide actionable insights to the utility managers for the seismic rehabilitation of their networks. Furthermore, a few models that actually provide some rehabilitation decision-support are limited by their simplifications and the use of sub-optimal optimization techniques. In this regard, this research was conducted to integrate a genetic algorithm-based optimization with a component-level seismic vulnerability assessment model and hydraulic modeling of the pipe network to identify critical pipes for proactive seismic rehabilitation of water pipe networks when utilities can only rehabilitate a finite length of pipes, to integrate a simulated annealing-based optimization with a component-level seismic vulnerability assessment model and hydraulic modeling of the pipe network to identify critical pipes for proactive seismic rehabilitation of water pipe networks when

utilities have a limited budget for rehabilitation, and to evaluate the performance of a wide range of resilience metrics for optimization of seismic rehabilitation of water pipe networks.

The results of this research show that the metaheuristic-based optimization methods such as genetic algorithm and simulated annealing demonstrate a really good performance when used to formulate an optimized policy for the seismic optimization of the water pipe network when the rehabilitation is subject to rehabilitation constraints. The results also shown that the metaheuristic-based optimization demonstrate superior performance when compared to the results of the latest methodology in literature. The results also show that the use of some graph theory based objective functions to maximize the post-earthquake serviceability of water pipe network can help reduce significant runtime of the optimization and can be used as surrogates for the computationally intensive hydraulics-based objectives.

The outcomes of this research offer novel contributions to field of decision science regarding the optimized seismic rehabilitation of water pipe network. Similarly, the outcomes are also valuable additions to the state practice since the resulting models can be highly useful to the utility managers for maximizing the post-earthquake serviceability of water pipe networks when the managers invest in the seismic rehabilitation of the water pipe networks.

TABLE OF CONTENTS

LIST OF TABLES

LIST OF FIGURES

CHAPTER 1

INTRODUCTION

Past earthquakes, such as the 1906 San Francisco earthquake, the 1994 Northridge, the 1995 Hyogoken-Nanbu (Kobe) earthquakes, and more recent earthquakes, such as the 2007 Niigata Chuetsu-Oki earthquake, the 2011 Christchurch earthquake, the 2011 East Japan earthquake, 2015 Gorkha earthquake, and Central Mexico earthquake (2017) have demonstrated that water pipe networks are extremely vulnerable to earthquakes (Cubrinovski et al. 2011; Hwang et al. 1998; Knight 2017; Maruyama et al. 2011; Thapa et al. 2016; Yasuda et al. 2012). Earthquake impacts on water supply networks can result in enormous direct losses (e.g., cost of repair) and indirect losses (e.g., disruption in water distribution) (Yerri et al. 2017) and severely limit capacity to control conflagrations following earthquakes (Selina et al. 2008). These facts highlight the significance of seismic vulnerability assessment of water pipe networks and mitigation of such vulnerabilities. A seismic vulnerability assessment of water supply networks estimates the likelihood of damage to pipelines and degradation of service after seismic events. The probabilistic nature of losses following earthquakes, complex network topology, a wide range of pipe materials, and different pipe and soil characteristics make seismic vulnerability assessment challenging. Several seismic vulnerability assessment models have been proposed to address these challenges. Despite all these models and technological advancements, water utility managers are often limited in what they can do, even when their budget allows additional maintenance. For example, if their budget will only cover the cost of inspecting or rehabilitating 1000 feet of large-diameter pipes, the water utility management must decide which pipe sections should be selected for rehabilitation. To address this, a methodology is required which can identify the critical pipes in water pipe

networks by considering criticality of the pipes along with limited rehabilitation resources of the utilities.

Hence, this research was conducted to integrate a genetic algorithm-based optimization with a component-level seismic vulnerability assessment model and hydraulic modeling of the pipe network to identify critical pipes for proactive seismic rehabilitation of water pipe networks when utilities can only rehabilitate a finite length of pipes, to integrate a simulated annealing-based optimization with a component-level seismic vulnerability assessment model and hydraulic modeling of the pipe network to identify critical pipes for proactive seismic rehabilitation of water pipe networks when utilities have a limited budget for rehabilitation, and to evaluate the performance of wide range of resilience metrics and their suitability as objective function for optimization of seismic rehabilitation of water pipe networks.

Chapter 2 provides a comprehensive literature review. This chapter first reviews current state of knowledge and practice regarding seismic vulnerability analysis of networked infrastructure and then focusses on the seismic vulnerability of analysis of water pipe networks. Finally, it discusses the optimized seismic rehabilitation of water pipe networks. Chapter 3 explains the methodology used to create a genetic algorithm-based optimization for proactive seismic rehabilitation of water pipe networks when utilities can only rehabilitate a finite length of pipes. Chapter 4 explains methodology used to create a simulated annealing-based for proactive seismic rehabilitation of water pipe networks when utilities have a limited budget for rehabilitation. Chapter 5 presents the methodologies that will be used to evaluate the performance of a wide range of resilience metrics and their suitability as objective function for optimization of seismic rehabilitation of water pipe networks. Chapter 6 presents that will be used to evaluate the performance of different approaches in decreasing optimization runtime. Finally, conclusions are presented in Chapter 7.

CHAPTER 2

BACKGROUND

In this section, we initially discuss the current literature dealing with vulnerability assessment of networked infrastructure systems and methodologies with synergistic applications. Then, we discuss the literature dealing with vulnerability assessment of water pipe networks considering non-seismic/generic hazards. Lastly, we focus on the works dealing particularly with the seismic vulnerability of buried pipe networks.

Pipe network is one of the "lifeline" networks which perform the critical function of providing access to the drinking water, transportation, electric power, and transportation services (Reed et al. 2009). Despite their critical function, such networks are vulnerable to an array of natural and man-made threats such as earthquakes, flooding, hurricanes, accidents, and human threats (Bonneau and O'Rourke 2009). Extensive research has been done to quantify the vulnerabilities of infrastructure systems to these threats and to mitigate them. Due to the complexity and the interdependency of these infrastructure systems, synergistic application of multi-disciplinary ideas is usually needed to model these systems. Infrastructure systems are typically modeled as networks comprised of nodes and links (Eusgeld et al. 2009; Ouyang 2014) and analyzed primarily using topological analysis and flow-based analysis. Topological analysis use graph theory and topological measures to study the vulnerability of wide variety of infrastructure systems such as electrical power systems (Crucitti et al. 2005; Rokneddin et al. 2009), and transportation systems (Angeloudis and Fisk 2006; Berche et al. 2009; Chen et al. 2007). In contrast, flow-based analyses utilize physics-based equations to quantify the vulnerabilities of transportation networks (Pandey et al. 2019; Sapkota et al. 2019b; a; Sullivan et al. 2010), natural gas distribution system (Han and Weng 2010), and wireless networks (Huang et al. 2007).

Topological and flow-based approaches are used to assess the vulnerability of water pipe networks as well. Grigg (2003) and Haimes et al. (1998) reviewed various threats, natural and man-made and identified various vulnerabilities of water pipe networks. Apostolakis and Lemon (2005) used graph theory and value tree to yield a prioritized list of scenarios induced due to the terrorist attack on water supply system. Yazdani and Jeffrey (2011) used several topological metrics to formulate resilience-enhancing expansion strategies for water pipe network. Gutiérrez-Pérez et al. (2013) used "Page Rank" and "HITS" algorithm combined with graph theory to identify critical zones in a water supply network. These topology-based methods are economical in terms of computational resources when solving a relatively large network. However, these models are inferior to flow-based models when predicting the system level serviceability of the network (Cavalieri et al. 2014). Hence, many other researchers used flow-based network models to assess the vulnerability of water network system. Murray et al. (2004) discussed the development of a probabilistic flow-based model by the United States Environmental Protection Agency (US EPA) to assess the vulnerability of water distribution system to broad range of contamination attacks. Shuang et al. (2014) used hydraulic simulation to study the nodal vulnerability of water pipe networks subjected cascading failure due to intentional attacks.

Significant literature exists in the field of seismic vulnerability of buried water pipe networks and can be broadly classified into two categories: component-level seismic vulnerability assessment models and system-level seismic vulnerability assessment models. Component-level seismic vulnerability assessment models evaluate the seismic performance of individual components of water pipe networks such as a single pipe or a single joint. System-level seismic vulnerability assessment models evaluate the seismic performance of the entire water pipe network and performance metrics of the entire network is monitored in such assessment. Early seismic

vulnerability assessment methods were mostly component-level vulnerability assessment methods that focused on the seismic performance individual water pipes. Many analytical component-level seismic vulnerability assessment models of buried pipes were developed. These models are summarized in Datta (1999). Despite the accuracy of such analytical models in estimating the actual stresses and strains induced in pipes due to earthquakes, these models require very accurate and wide-ranging data which is usually unavailable to the utilities. Few data that is available is prone to uncertainties and yield inaccurate results if the data is used without some data-fusion-based processing (Shahandashti et al. 2010). However, empirically derived seismic vulnerability relations for buried pipes (American Lifelines Alliance (ALA) 2001; Honegger and Eguchi 1992; Jeon and O'Rourke 2005; O'Rourke and Ayala 1993) are typically used in system-level vulnerability assessment.

During the past two decades, advances in computational engineering, probabilistic modeling, and network simulation have motivated researchers to go beyond component-level assessments and create seismic vulnerability assessments of water pipe networks, i.e. system-level seismic vulnerability assessment models. These existing component-level and system-level seismic vulnerability assessment methods for water pipe networks are reviewed here. Markov et al. (1994) developed Graphical Interactive Serviceability Analysis of Lifelines subjected to Earthquake (GISALLE) to evaluate the seismic performance of Auxiliary Water Supply System of San Francisco. Markov et al. (1994) only considered pipe breaks in their model and ignored pipe leaks. However, this is not realistic as most of the damages (80%) due to seismic ground shaking is realized as leaks (Ballantyne and Taylor 1990). Hwang et al. (1998) proposed a GIS-based method to study post-earthquake serviceability of water supply system considering probabilistic leaks and breaks. Shi (2006) built on the work of Markov et al. (1994) and created a computer code called

Graphical Iterative Response Analysis for Flow Following Earthquakes (GIRAFFE). GIRAFFE uses empirical seismic vulnerability functions proposed by Jeon and O'Rourke (2005) and Monte Carlo simulation to simulate random, earthquake-induced, pipe damages in the network. Monte Carlo simulation is often used in probabilistic simulation-based studies to account for the uncertainty in the underlying processes (Abediniangerabi et al. 2018; Shahandashti et al. 2017). Shi (2006) also refined hydraulic models of leaks and breaks previously used (Ballantyne and Taylor 1990; Hwang et al. 2004; Markov et al. 1994) and incorporated it in GIRAFFE to perform accurate hydraulic analysis of water pipe network damaged by an earthquake. GIRAFFE was then used to study the seismic response of Los Angeles Department of Water and Power (LADWP) during Northridge earthquake of 1994. However, Shi (2006) did not propose any method of identifying proper rehabilitation measures to reduce the seismic vulnerability of the system and was focused solely on the seismic vulnerability assessment of water supply systems. Takao Adachi (2007) and Adachi and Ellingwood (2008) proposed a method to analyze the post-earthquake serviceability of water supply system considering its interdependency with the electrical power distribution system using fault tree analysis and shortest path algorithm. Their work also highlighted the need to consider spatial correlation and scenario earthquake when analyzing the seismic vulnerability of spatially distributed systems. However, their work ignored the hydraulics (i.e., flows and pressures) of the water pipe systems and considered only the post-earthquake connectivity of the system to evaluate seismic vulnerability of water pipe network. Wang et al. (2010) introduced the System Serviceability Index (SSI) for a water pipe network subjected to earthquakes. Theses indices combined with the efficient frontier approach were used to identify and rank the network's critical pipes. The System Serviceability Index (SSI), as per Wang et al. (2010), is defined as the ratio of water demand fulfilled after an earthquake to the inherent

(original) demand of the water pipe network. Zohra et al. (2012) proposed an index for prioritizing pipes in a water supply network. The index is based on the pipe diameter, seismic intensity, and soil conditions. However, hydraulics and network topology are not considered in this index.

From the above discussion, it can be concluded that most of the literature dealing with the seismic vulnerability of water pipe networks are focused on the estimating the response of the water pipe networks to earthquakes; very few of them go beyond that and provide some actionable insights to the utility managers to perform some seismic rehabilitation of their water pipe networks. Despite existence of several literature dealing with investment evaluations under uncertainty for other infrastructure systems (Kashani et al. 2012; Zahed et al. 2017), similar do not exist for the water supply systems.

2.1 Problem Statement

Water utilities cannot perform seismic rehabilitation of an entire network due to budget limitations. They must identify a few critical pipes and invest in their seismic rehabilitation to enhance the network's post-earthquake serviceability (Klise et al. 2015). Currently, utility managers are struggling to find a comprehensive model that can identify critical pipes for seismic rehabilitation. However, most of the models (Adachi 2007; Hwang et al. 1998; Shi 2006; Zolfaghari and Niari 2009) only propose approaches for seismic vulnerability assessment of water pipe networks but do not recommend any methods to mitigate these vulnerabilities. A few simple prioritization models (Fragiadakis and Christodoulou 2014; Wang et al. 2010; Zohra et al. 2012), based on seismic vulnerability, are proposed in the literature to identify critical pipes for seismic rehabilitation despite existence of other powerful and more appropriate meta-heuristic based optimization solvers (Chen and Shahandashti 2007, 2009, 2008; Juan et al. 2015). Fragiadakis and Christodoulou (2014) and Zohra et al. (2012) ignored hydraulics of the problem when

recommending critical pipes. Wang et al. (2010) oversimplified the seismic vulnerability assessment by using a uniform peak ground velocity for the entire network when identifying critical links. This leads to underestimation of seismic hazard, especially for spatially distributed systems such as water pipe networks (Adachi 2007; Weatherill et al. 2013; Zanini et al. 2016). Furthermore, none of the discussed models, consider the limited rehabilitation resource constraint and system level distribution of this limited resources and therefore, cannot find an economical solution. Hence, as such, following gaps in literature can be identified in the current literature:

- Current methods in literature do not integrate a metaheuristic-based optimization algorithm with a component-level seismic vulnerability assessment model and hydraulic modeling of the pipe network.

- Current literature does not have a comprehensive study that evaluates performance of resilience metrics and their suitability as objective function for optimization of seismic rehabilitation of water pipe networks.

2.2 Objectives

The broad objective of the current research is to develop an approach for identifying pipes that are most critical to the proactive seismic rehabilitation of water pipe networks for enhancing post-earthquake serviceability. The broad objectives can be broken down into the following specific objectives:

- To integrate a genetic algorithm-based optimization with a component-level seismic vulnerability assessment model and hydraulic modeling of the pipe network to identify critical pipes for proactive seismic rehabilitation of water pipe networks **when utilities can only rehabilitate a finite length of pipes**,

- To integrate a simulated annealing-based optimization with a component-level seismic vulnerability assessment model and hydraulic modeling of the pipe network to identify critical pipes for proactive seismic rehabilitation of water pipe networks **when utilities have a limited budget for rehabilitation**, and

- To evaluate the performance of wide range of **resilience metrics and their suitability as objective function for optimization** of seismic rehabilitation of water pipe networks.

2.3 Research Plan

To achieve the set-out objectives, the research plan is divided into following tasks:

Task 1: Create a genetic algorithm-based optimization for proactive seismic rehabilitation of water pipe networks when utilities can only rehabilitate a finite length of pipes

Task 2: Create a simulated annealing-based for proactive seismic rehabilitation of water pipe networks when utilities have a limited budget for rehabilitation

Task 3: Evaluate the performance of a wide range of resilience metrics and their suitability as objective function for optimization of seismic rehabilitation of water pipe networks.

The methodology and results associated with each of these tasks are presented in chapter 3, chapter 4, and chapter 5 of this dissertation.

CHAPTER 3

OPTIMIZED PROACTIVE SEISMIC REHABILITATION OF WATER PIPE

NETWORKS SUBJECT TO LENGTH CONSTRAINT

This chapter explains the methodology adopted to create a genetic algorithm-based optimization for proactive seismic rehabilitation of water pipe networks when utilities can only rehabilitate a finite length of pipes. The methodology can be divided into following two sub-tasks:

1) Formulation of stochastic combinatorial optimization to maximize post-earthquake serviceability of water pipe networks where rehabilitation is constrained by the ability of the utilities to rehabilitate only a limited length of pipes.

2) Solving the stochastic combinatorial optimization by integrating a genetic algorithm with the network-level seismic vulnerability assessment to identify critical pipes for proactive seismic rehabilitation.

3.1 Formulation of Stochastic Combinatorial Optimization

The problem was defined as the maximization of the expected value of the System Serviceability Index (SSI) of a water pipe network if water agencies can only rehabilitate a limited length of pipes (l_{rehab}) due to budget limitations. Equation 3-1 presents the objective function.

$$\max_{x \in X} E[SSI(x)] \qquad\qquad (3\text{-}1)$$

where X represents the set of all the rehabilitation policies (x). Here, a rehabilitation policy (x) is created by choosing two outcomes: "rehabilitation" or "no rehabilitation", for each pipe in the network. Let us consider a network with two pipes. A rehabilitation policy for this network can be represented by a set $\{x_1, x_2\}$ where $x_i = 1$ represents i^{th} pipe is rehabilitated and $x_i = 0$ means i^{th} pipe is not rehabilitated. Based on this, the set of all rehabilitation policy for this network would

be X = {{0,0}, {0,1}, {1,0}, {1,1}}. As such, without any feasibility constraints, $X \in \mathbf{B}^{2^{N_p} \times N_p}$ which is a combinatorial decision space where N_p is the total number of pipes in the network. However, the size of **X** is reduced by the feasibility constraint imposed by the condition that any rehabilitation policy ($\mathbf{x} \in \mathbf{X}$) cannot suggest rehabilitating pipes longer than l_{rehab}. As a proof of concept, we have used the rehabilitation length constraint as the only constraint in this study. However, the proposed model is flexible enough to accommodate any other constraints, such as always rehabilitating a set of pipes or not rehabilitating a set of pipes.

The calculation of the SSI involves solving many nonlinear hydraulic equations that require knowledge of the location and magnitude of earthquake-induced damage (pipe leaks and pipe breaks). The properties of earthquake-induced damage are probabilistic, due to aleatory uncertainties, making the SSI a probabilistic quantity. Thus, the probabilistic nature of the SSI, along with the combinatorial nature of the selection of pipes for seismic rehabilitation, makes the problem a stochastic combinatorial optimization. Hence, a solution of the formulated problem will entail solution of stochastic combinatorial optimization.

3.2 Solution Methodology

Solving the stochastic combinatorial optimization problem is extremely challenging due to non-convex and non-continuous objective function and the lack of closed-form representation for the objective function. Since the objective function does not necessarily have a closed-form representation, conventional algorithms for solving combinatorial stochastic optimization problems, such as deterministic reformulation, are not applicable. Therefore, a genetic algorithm (Holland 1975) was devised and integrated with the seismic vulnerability assessment of water pipe networks. The integrated genetic algorithm identifies which pipes in a water pipe network are critical for proactive seismic rehabilitation to maximize the post-earthquake serviceability of water

pipe networks. The maximization is constrained by the water agencies' inability to rehabilitate all the pipes due to infrastructure funding gaps (US EPA 2002). Figure 3-1 shows how the genetic algorithm is integrated with the seismic vulnerability assessment of water pipe networks.
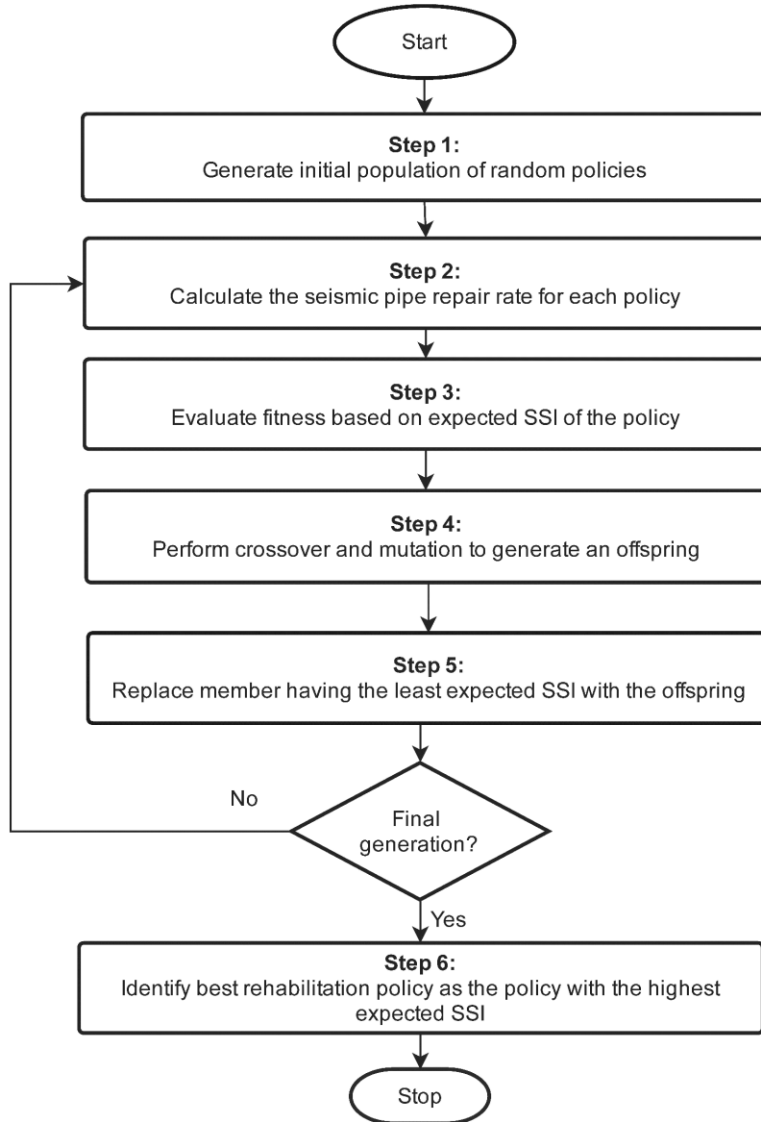
Figure 3-1 Genetic algorithm integrated with seismic vulnerability assessment of water pipe networks

Binary encoding was adopted to represent rehabilitation policies, i.e., chromosomes of the genetic algorithm. Each rehabilitation policy (x) was represented by a binary vector, so that each element of the binary vector represented a rehabilitation decision for a specific pipe. (0 and 1 indicate no rehabilitation, and rehabilitation for a pipe, respectively.) For example, assume a water pipe network with five pipes. A rehabilitation policy of rehabilitating the first and last pipe for this network would be represented by the binary vector [10001]. These vectors are referred to as solution vectors in this study.

While generating solution vectors, the following constraint was used to discard solutions:

$$\sum_{k=1}^{N_p} a_k l_k \leq l_{rehab} \tag{3-2}$$

where a_k is 1 if pipe k is rehabilitated, a_k is 0 if pipe k is not rehabilitated, N_p is number of pipes in the network, and l_k is the length of pipe k.

The algorithm begins with an initial population generation, which involves the creation of five random solution vectors that represent five random rehabilitation policies. This initial population acts as the current generation at the start of the genetic algorithm. The mutation rate of the genetic algorithm is initialized at 0.9 at the start of the algorithm.

Following the initialization of parameters of the genetic algorithm, seismic pipe repair rates were calculated. ALA defines seismic pipe repair rate as the expected pipe repairs per 304.8 m. (1000 ft.) of pipe following an earthquake. Thus, the seismic pipe repair rate indicates the number of expected leaks and breaks in a pipe following an earthquake and is determined based on the peak ground velocity at the location of the pipe, the structural properties of the pipes, and the corrosivity of soil. The method of calculating the seismic pipe repair rate is illustrated in Figure 3-2
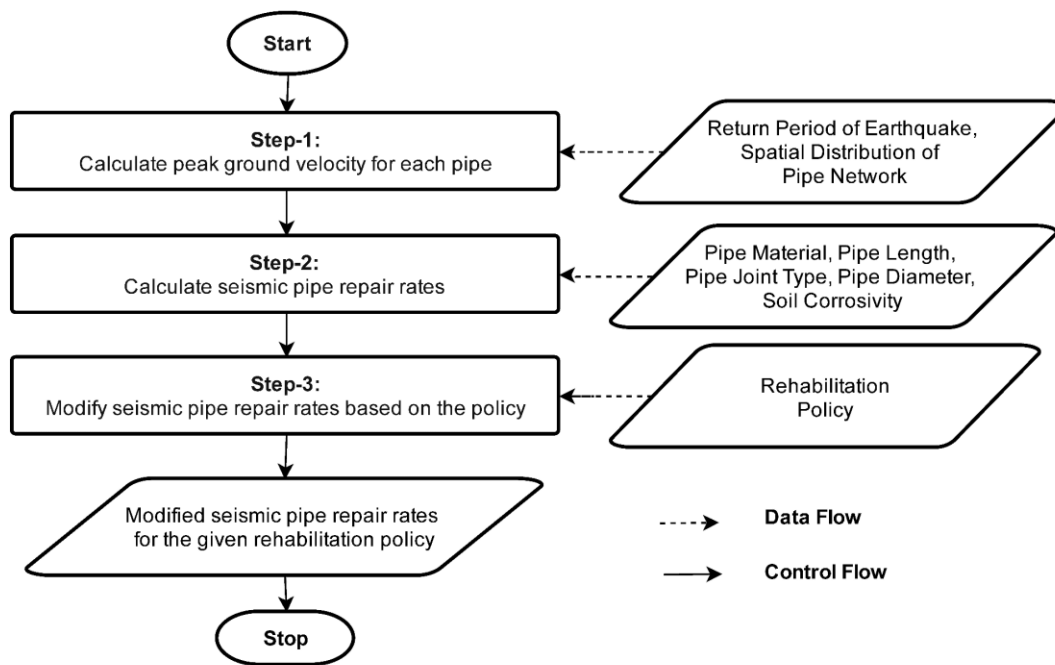
Figure 3-2. Seismic pipe repair rate calculation

The calculation of the seismic pipe repair rate starts with the selection of a scenario earthquake subjected to which the expected SSI of a water pipe network should be maximized. Scenario earthquakes are typically used for seismic analysis of utilities because modeling earthquakes as scenarios allows consideration of spatial correlation between seismic intensities which cannot be ignored for spatially distributed infrastructure like water pipe networks, transportation networks, and spatially distributed portfolio of structures (Adachi 2007; Weatherill et al. 2013; Zanini et al. 2016, 2017). Moreover, results from scenario earthquakes are easier to communicate with non-specialist decision makers (Adachi 2007). Hence, for this study, we use a scenario earthquake selected based on deaggregation analysis proposed by Adachi (2007). Based on this method, a return period is selected based on utility's resources and utility's risk tolerance. The selected return period is then used to generate deaggregation maps for 1.0s spectral acceleration maps using

deaggregation tool developed by USGS (2018). Then, an earthquake with highest contribution ratio is selected as the scenario earthquake, for the analysis, from the list of characteristic earthquakes obtained from deaggregation analysis.

Next, the peak ground velocity and permanent ground deformation should be calculated for the selected earthquake. Peak ground velocity quantifies the maximum level of transient seismic ground shaking experienced at a given location during an earthquake. We select peak ground velocity as the seismic intensity parameter because peak ground velocity is directly related to the transient strains induced in the soil during an earthquake, which are the primary causes of failures of buried pipes, due to seismic ground shaking (Pineda-Porras and Najafi 2010).

Permanent ground deformation quantifies the expected level of earthquake-induced geotechnical instability, such as liquefaction, landslide, and lateral spreading at a given location following an earthquake. For this study, to focus on the effects of seismic ground shaking alone, it was assumed that the site was not susceptible to earthquake-induced geotechnical instability; hence peak ground displacement was assumed to be zero.

Following the selection of earthquake scenario, we choose Ground Motion Prediction Equation (GMPE) proposed by Abrahamson and Silva (2007) along with Zanini et al. (2016, 2017)'s approach to generate spatially correlated peak ground velocity field. The general expression for calculating peak ground velocity is given by

$$log_{10}(PGV_{ij}) = f(M_i, R_{ij}, \theta_i) + \sigma_B \nu_i + \sigma_W \varepsilon_{ij} \qquad (3\text{-}3)$$

where PGV_{ij} is the peak ground velocity for a site j, at a distance of R_{ij} from the source i during an earthquake event of magnitude M_i, θ_i is the geological parameters defining the fault at source

i, $\sigma_B \nu_i$ represents the residual inter-event variability whereas $\sigma_W \varepsilon_{ij}$ represents intra-event residual. Peak ground velocity map for the selected earthquake, without inter-event and intra-event variability i.e., $f(M_i, R_{ij}, \theta_i)$, was generated based on Abrahamson and Silva (2007). To incorporate the inter-event and intra-event variabilities in this map, ν_i and ε_{ij} were generated where ν_i and ε_{ij} are normally distributed random variables with mean ($\mu = 0$) and standard deviations σ_B and σ_W. However, ε_{ij} is spatially correlated as well. To consider this, we used the following equation based on Weatherill et al. (2013) and Zanini et al. (2016) to generate ε_{ij} such that

$$\varepsilon_{ij} = \mu + LZ \tag{3-4}$$

where μ is taken as 0, Z is the vector of random variable with standard normal distribution, and L is the lower triangular matrix, obtained using Cholesky decomposition method, such that $LL^T = C$, where C is positive-definite covariance matrix calculated as

$$C = \begin{bmatrix} 1 & \sigma(h_{1,2}) & \dots & \sigma(h_{1,N}) \\ & 1 & \dots & \sigma(h_{2,N}) \\ & & \ddots & \vdots \\ sym & & & 1 \end{bmatrix} \tag{3-5}$$

where $\sigma(h_{j,k})$ is correlation coefficient between intra-event residuals calculated for sites j, k, among total N sites, where $\sigma(h_{j,k})$ is calculated, based on Zanini et al. (2016) as:

$$\sigma(h_{j,k}) = e^{\left(\frac{-3h_{j,k}}{b}\right)} \tag{3-6}$$

where $h_{j,k}$ is the inter-site distance between sites j and k, b is the inter-site distance between which spatial correlation is negligible. Wang and Takada (2005) recommends the value of b within a

3-7

range of 20 km to 40 km, when the spatial correlation is calculated for peak ground velocity. Hence, for this study, b=30 km is used. *m* random peak ground velocity fields were generated by repeating this process *m* times Zanini et al. (2017). For each of these *m* fields, average peak ground velocity was calculated for each pipe. The average peak ground velocity was used because Adachi (2007) concluded that, using average peak ground velocity for each water pipe leads to a lower bound estimate of network serviceability, which is conservative from disaster planning perspective.

After the average peak ground velocity is calculated for each pipe, seismic repair rate is calculated by using the empirical seismic vulnerability relationship proposed by ALA (2001). The relationship is stated as:

$$RR_{k,m} = K1 * 0.00187 * PGV_m \quad \text{(For seismic ground shaking)} \tag{3-7}$$

where $RR_{k,m}$ is seismic repair rate per 304.8 m. (1000 ft.) of pipe k for m^{th} peak ground velocity field; PGV_m (measured in inches/second) is the average peak ground velocity for the pipe based on m^{th} peak ground velocity field; and $K1$ is the modification factor which adjusts the repair rate based on pipe material, diameter, pipe joint characteristics, and soil corrosivity. The values of $K1$ are tabulated in ALA (2001).

Seismic pipe repair rates thus calculated are referred as unmodified repair rates. Modified seismic pipe repair rates are calculated using Eq. (3-8) for each rehabilitation policy in the current generation of the genetic algorithm.

$$RR_k^{x,j} = RR_{k,j} * (1 - a_k^x) \tag{3-8}$$

where $RR_k^{x,j}$ is the modified seismic pipe repair rate for pipe k based on rehabilitation policy x and j^{th} peak ground velocity field, $RR_{k,j}$ is the seismic pipe repair rate for pipe k and j^{th} peak ground velocity field , a_k^x is 0 if the pipe is unrehabilitated based on policy x, and a_k^x is 1 if the pipe is rehabilitated based on policy x.

After the modified seismic pipe repair rate is calculated for each pipe in the network, expected SSI is calculated for the rehabilitation policy x. Calculation of expected SSI is required for the fitness evaluation of each rehabilitation policy in the current generation of the genetic algorithm. To accomplish this, a Monte Carlo simulation is devised to calculate the expected SSI (Figure 3-3).
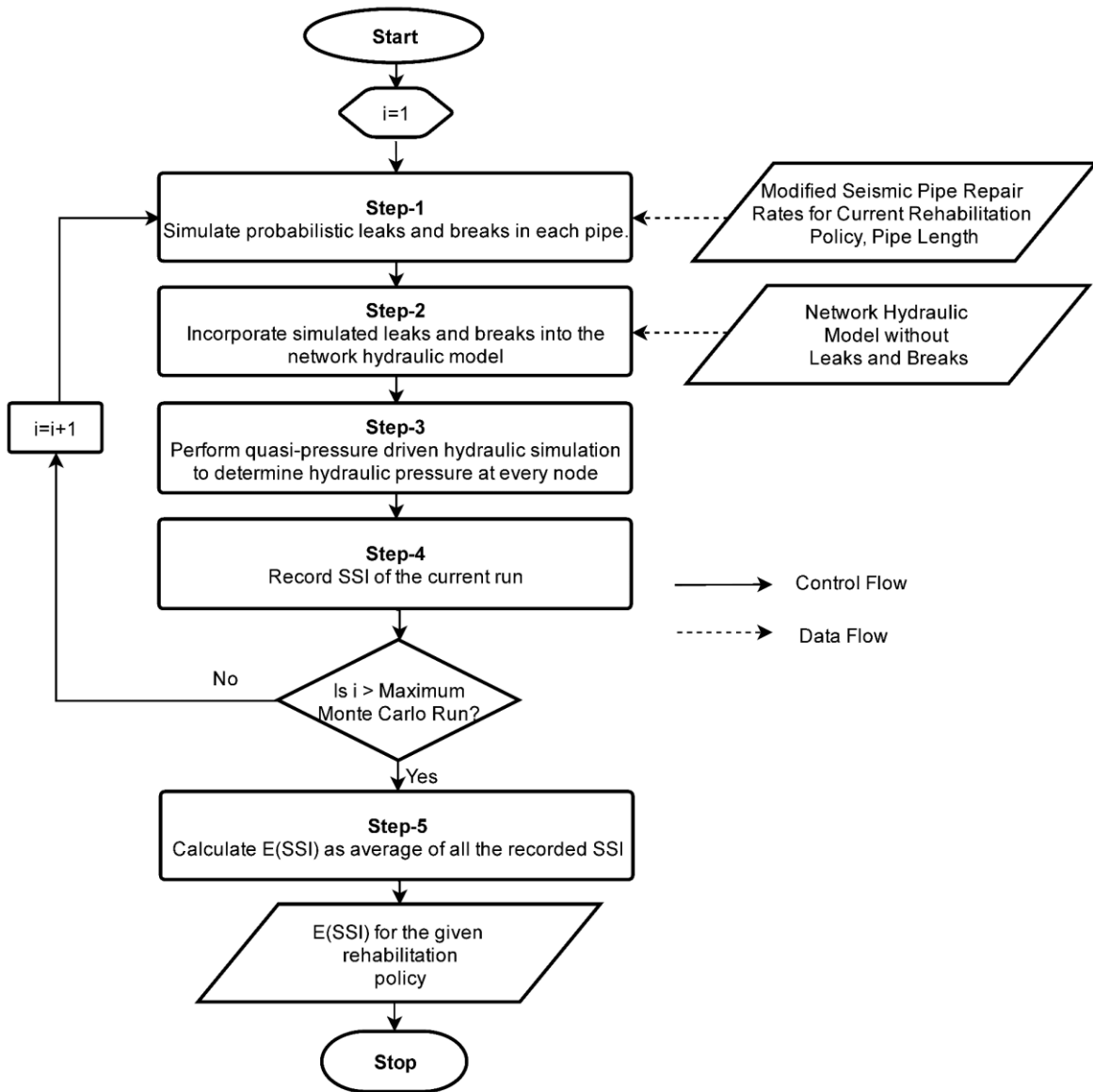
Figure 3-3. Expected system serviceability index calculation for a rehabilitation policy

The expected System Serviceability Index for a rehabilitation policy T is calculated as:

$$E[SSI(x = T)] = \frac{\sum_{j=1}^{m} \sum_{r=1}^{NMCS} \sum_{i=1}^{N} x_{ri}^{T,j} D_i}{m * NMCS * \sum_{i=1}^{N} D_i} \tag{3-9}$$

Subject to

$$x_{ri}^{T,j} = 1 \ if \ P_{ri}^{T,j} \geq P_{threshold}$$

$$x_{ri}^{T,j} = 0 \ if \ P_{ri}^{T,j} \leq P_{threshold}$$

where N is the number of nodes in the network, $NMCS$ is the number of Monte Carlo simulation runs adopted for evaluating each rehabilitation policy, D_i is the water demand at node i, $P_{ri}^{T,j}$ is the hydraulic pressure at node i during the rth run of Monte Carlo simulation for rehabilitation policy T for j^{th} peak ground velocity field, and $P_{threshold}$ is the minimum hydraulic pressure required at the node, imposed by the firefighting demand. In this study, a hydraulic pressure of 0.14 MPa (20 psi) was used as the $P_{threshold}$, as suggested by Trautman et al. (2013).

For a rehabilitation policy T, each run of the Monte Carlo simulation begins by determining the location of earthquake-induced leaks and breaks in the water pipe network. This is accomplished by modeling the earthquake-induced leaks and breaks as the Poisson process, where the location of the ith leak or break in a pipe P is determined by:

$$l_{P,i} = l_{P,i-1} - \frac{1}{RR_P^{T,j}} * \ln(1 - U) \quad where \quad l_{P,0} = 0 \qquad \text{(3-10)}$$

where $l_{P,i}$ is the distance of ith discontinuity (leak or break) in pipe P from its start node, $RR_P^{T,j}$ is the seismic pipe repair rate calculated for the pipe P based on policy T for the jth peak ground velocity field, and U is the uniformly distributed random number between 0 and 1. If the location of the first leak or break lies within the length of the pipe, i.e., $l_{P,1}$ is less than the length of pipe P, then a second random number is generated to classify it as either a leak or a break. If the second random number generated is less than or equal to 0.8, the discontinuity at the location $l_{p,1}$ is classified as a leak; otherwise, it is classified as a break (FEMA - Federal Emergency Management Agency 2013; Shi 2006). Leaks are further classified, and the diameters of the leaks are calculated

based on Shi (2006). This process is repeated for higher values of i until the value of $l_{p,i}$ exceeds the length of the pipe. The same process is repeated for other pipes in the network.

After all of the leaks and breaks have been located and the diameters of all of the leaks have been determined for the current Monte Carlo run, they are integrated into the network hydraulic model of the undamaged water pipe network. The hydraulic modeling of leaks and breaks proposed by Shi (2006) is used for this integration. The resulting hydraulic model is then analyzed, using a quasi-pressure-driven hydraulic analysis, to determine the hydraulic pressures at each node (P_{ri}^T). This analysis is required because conventional demand-driven hydraulic analysis assumes that the hydraulic demand at each node is always fulfilled, and that may not be a valid assumption for water pipe networks damaged by an earthquake (Cheung et al. 2005; Ozger and Mays 1994, Shi 2006). Hydraulic analysis, with the assumption that nodal water demand is not always fulfilled, and that the system can have no negative pressure in the nodes, is more realistic. Therefore, for this study, the quasi-pressure-driven analysis approach was adopted, and the following operations were performed for each run of the Monte Carlo simulation:

1) Hydraulic model with integrated leaks and breaks was analyzed.

2) Nodes with negative pressure were identified and removed from the network.

3) Step 1 and step 2 were repeated until there were no nodes with negative pressure.

Using this approach, the hydraulic pressure at each node (P_{ri}^T) was calculated and recorded for a predefined maximum number of Monte Carlo runs (NMCS) for the rehabilitation policy ($x=T$). The expected serviceability index of the water pipe network for a rehabilitation policy($x=T$) in the current generation of genetic algorithm was calculated, using Eq. (3-9). The entire process was repeated for other rehabilitation policies until the expected serviceability index of every rehabilitation policy in the current generation of genetic algorithm was determined.

Next, to advance to the next generation of the genetic algorithm, genetic operations as proposed by Chen and Shahandashti (2009) were used for this research. All the policies in the current generation were ranked, based on their expected SSIs, and the two policies with the highest expected SSIs were selected to produce an offspring policy. A two-point crossover followed by random mutation of 20% of the offspring was performed on the offspring policy. The crossover and mutation operation were repeated until the cumulative rehabilitation length represented by the mutated offspring was less than or equal l_{rehab}.

Subsequently, the current generation's rehabilitation policy with the least expected SSI was replaced by the offspring. This replacement yielded a new current generation of genetic algorithms. Subsequently, the generation number was increased and checked for exceedance of the maximum generation number. If no exceedance occurred, then for the next generation, the mutation rate was decreased by 3%. This process of expected SSI calculation and the genetic operation was repeated for new current generation until the maximum generation was reached. The rehabilitation policy with highest expected SSI in the last generation represented the best seismic rehabilitation policy for the selected earthquake, given water pipe network, and the given rehabilitation budget constraints. The pipes chosen for seismic rehabilitation were identified as the critical pipes in the water pipe network.

3.3 Results

To demonstrate the application of the approach created in this study, we used a benchmark network called Modena network (Figure 3-4), from Center of Water Systems (2018). This network was created for resilience study of large dimensional water pipe network. The network has 268 junctions, 317 pipes, and four reservoirs with fixed head within 72.0 m to 74.5 m. The total length of the pipes of the entire network is 71806.11 m. For the calculation of seismic repair rate, pipes

with diameter less than 300 mm (12 inches) were considered as Cast-Iron pipes with lead joints while pipes with diameter greater than 300 mm (12 inches) were considered as Ductile-Iron (DI) pipes with rubber gasketed joints.
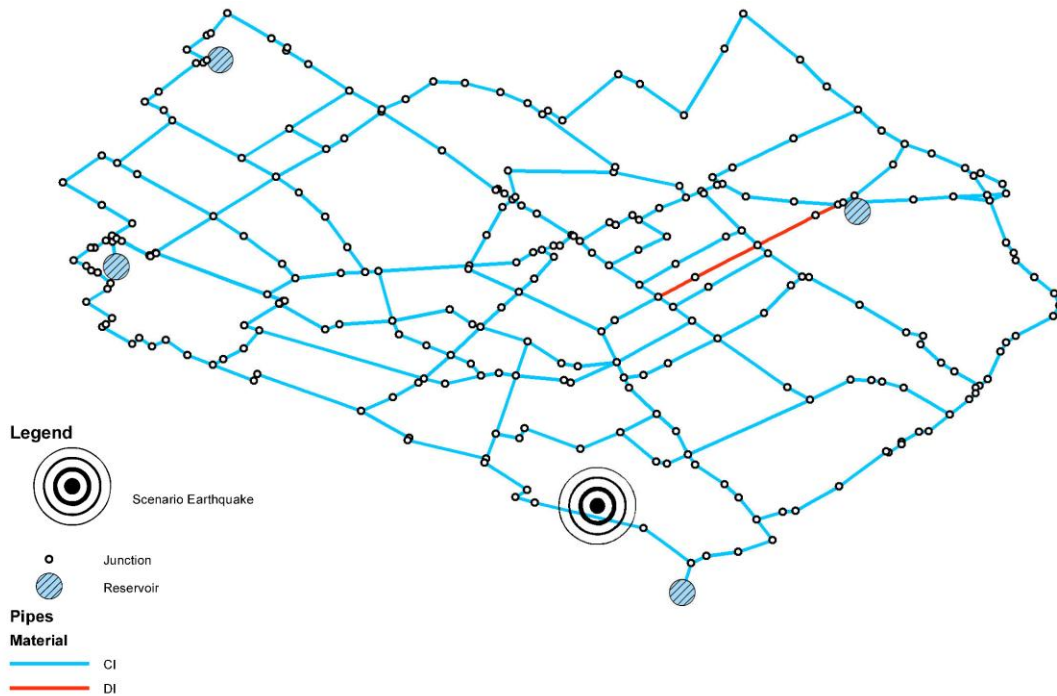
Figure 3-4.. Modena Network

For the seismic vulnerability analysis, the location of the centroid of the network was assumed to be Pasadena, California (34.146267° N, 118.144040 W). A deaggreagation analysis was performed at 34.146267° N , 118.144040 W for 1.0 s spectral acceleration for the return period of 2475 years using USGS (2018). From the deaggregation result, an earthquake originating at Raymond fault, 3.25 km from the network's centroid, with a magnitude of 7.12 was identified with maximum contribution ratio (13.84%). This was selected as the scenario earthquake for this study. Subsequently, peak ground velocity field due to the scenario earthquake without inter-event and intra-event variability was generated based on Abrahamson and Silva (2007) around the network.

Grid of 0.1° was used for generating this field. The generated peak ground velocity field is shown in Figure 3-5 and Figure 3-6. The fault parameters used to generate the field was obtained from SCEDC (2018) and USGS (2018b). An average peak ground velocity was calculated for each pipe. These were then used to calculate expected SSI of the network using Eq. (3-9) for each rehabilitation policy. Using the Monte Carlo simulation, the expected SSI of the network without any rehabilitation was calculated as 0.789 for the scenario earthquake. The devised algorithm was then used to calculate the best seismic rehabilitation policy, and consequently the critical pipes, for different rehabilitation constraints. Table 3-1 shows the parameters of the genetic algorithm, while Table 3-2 summarizes the results. The critical pipes identified by the devised approach for different rehabilitation constraints are marked as thick green lines in Figure 3-7. Figure 3-7 shows the critical pipes for rehabilitation with lengths less than or equal to 15% (Figure 3-7-a), 20% (Figure 3-7-b), 25% (Figure 3-7-c), 30% (Figure 3-7-d), 35% (Figure 3-7-e), 40% (Figure 3-7-f), 45% (Figure 3-7-g), and 50% (Figure 3-7-h), of the total pipe length.

Table 3-1. Genetic Algorithm Parameters

GA Parameter	Values
Maximum Generation	50
Initial Mutation Rate	90%
Cross Over Type	2 Point Cross Over
Decrease of Mutation Rate	3% every generation
Number of bits mutated	20% of chromosome=24 bits

Legend

 Scenario Earthquake

 Network CG
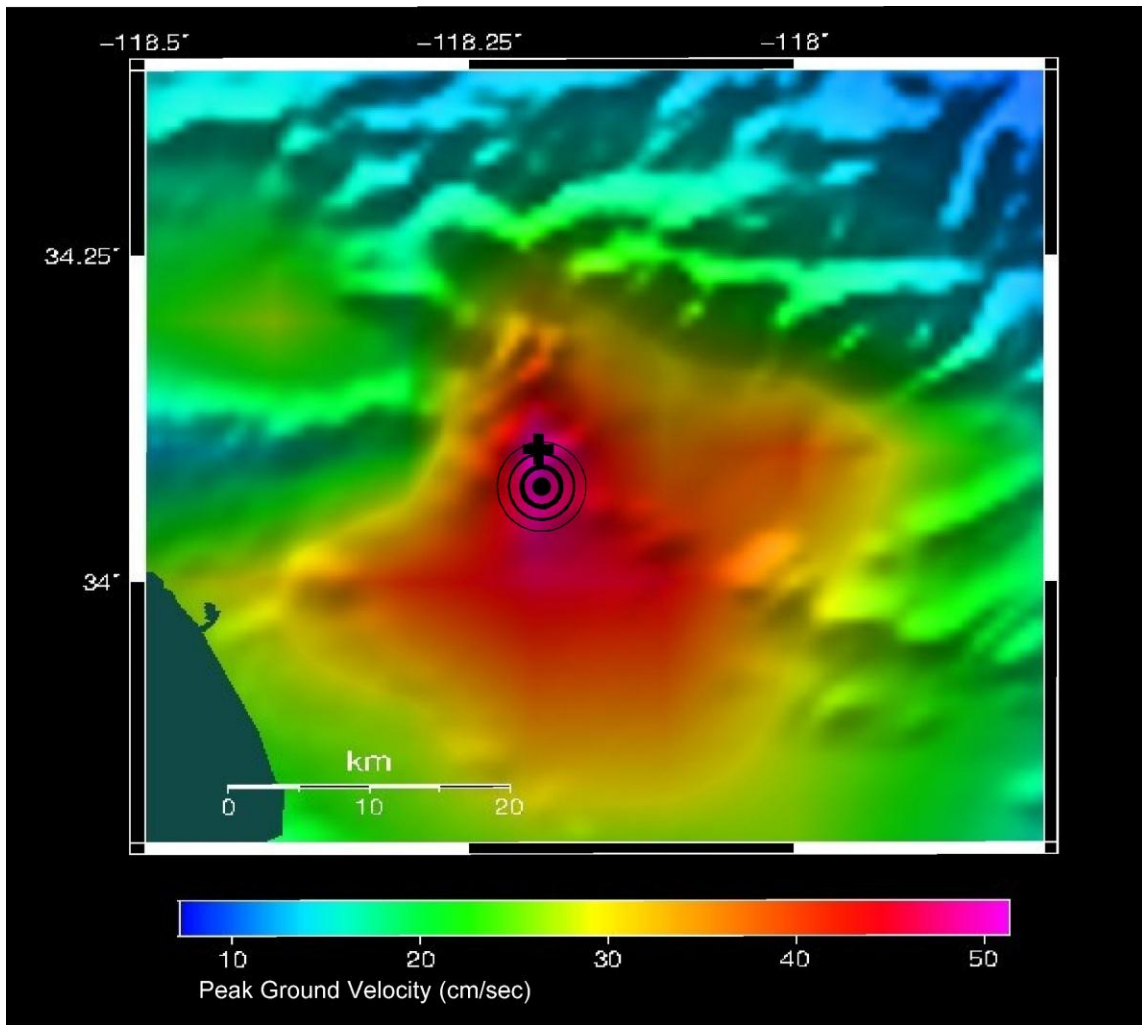
Figure 3-5. Peak ground velocity field due to the selected earthquake scenario
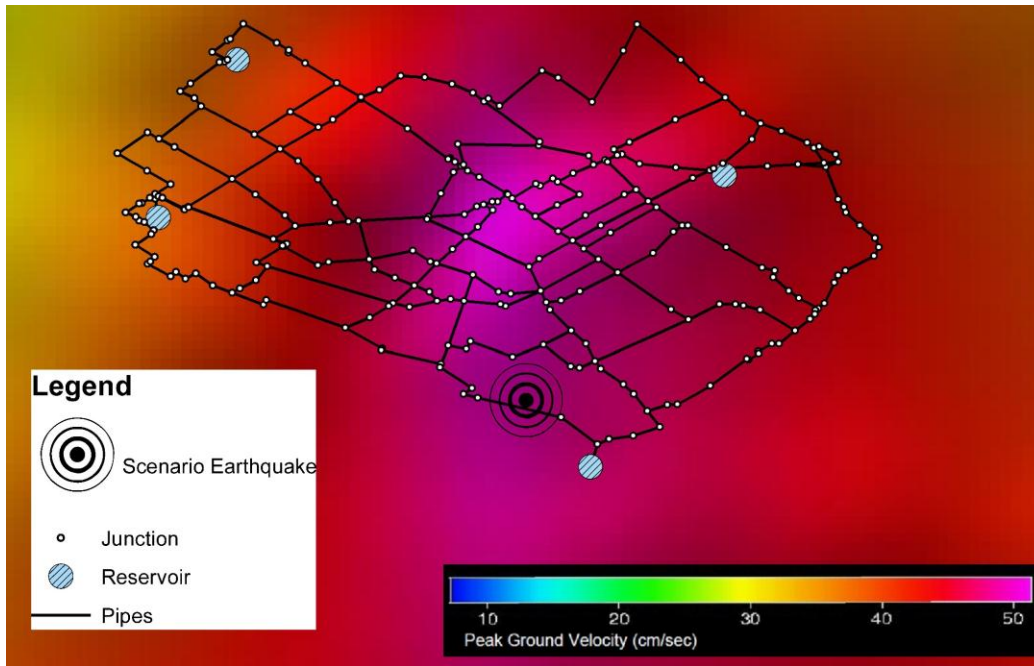
Figure 3-6. Peak ground velocity field due to the selected earthquake scenario
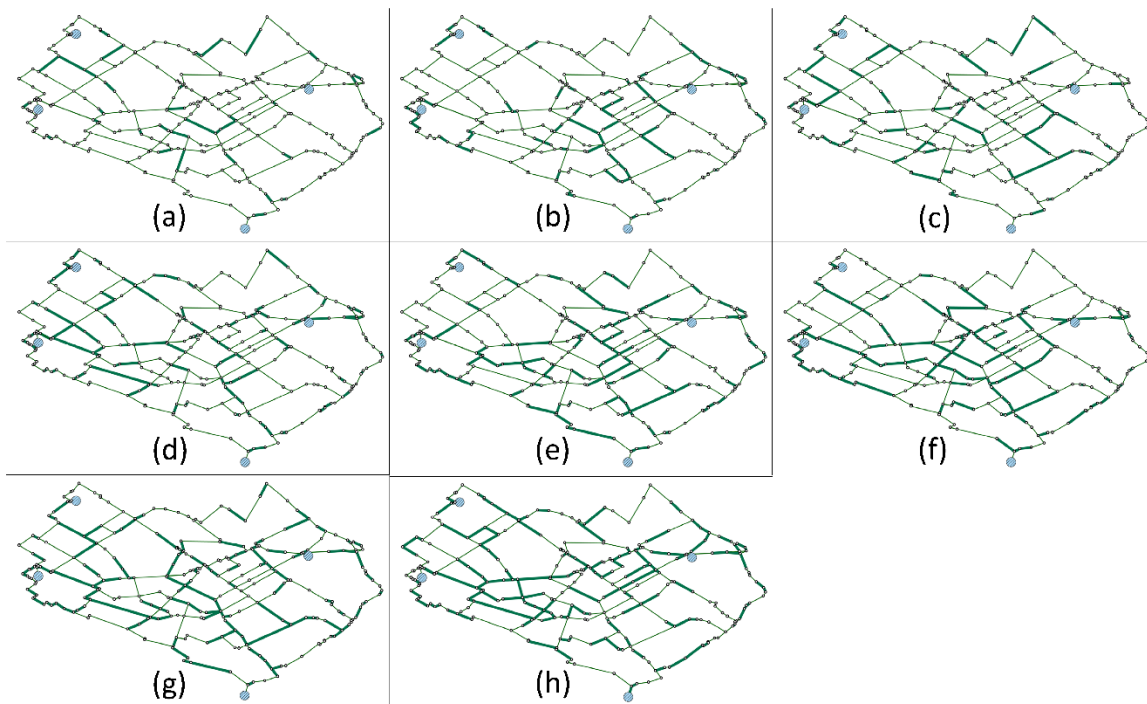
Figure 3-7. Critical pipes identified by the devised approach for Modena network

Table 3-2. Results based on the proposed approach for different rehabilitation length constraints

for Modena network

Percentage of total pipe length allowed for rehabilitation	Percentage of total pipe length actually rehabilitated	Expected SSI	Variance
Not more than 15	13.553	0.8377	0.0289
Not more than 20	19.648	0.8557	0.0245
Not more than 25	23.859	0.8669	0.0249
Not more than 30	29.401	0.8864	0.0206
Not more than 35	34.813	0.8997	0.0167
Not more than 40	38.359	0.9103	0.0185
Not more than 45	43.697	0.9293	0.0111
Not more than 50	49.334	0.9313	0.0117

3.3.1 Validation

For validation, a simple rehabilitation scheme was considered, based on pipe length, wherein the longer pipes were identified as the critical pipes. This scheme was combined with different rehabilitation length constraints, as shown in Table 3-3, to identify critical pipes for seismic rehabilitation. The critical pipes identified by this simple prioritization scheme are highlighted

green in Figure 3-8, and the results obtained for this scheme are summarized in Table 3-3. Figure 3-8 shows the critical pipes that were identified using this approach, when the length was less than or equal to 15% (Figure 3-8-a), 20% (Figure 3-8-b), 25% (Figure 3-8-d), 35% (Figure 3-8-e), 40% (Figure 3-8-f), 45% (Figure 3-8-g), and 50% (Figure 3-8-h), of the total pipe length. When the expected SSI for each of these cases (Table 3-3) was compared with the expected SSIs obtained by using methodology created in this study for respective rehabilitation constraint (Table 3-2), it was clearly seen that the expected SSI of the policy identified by the devised methodology was greater than the expected SSI of the policy based on the simple prioritization scheme for respective rehabilitation constraint.
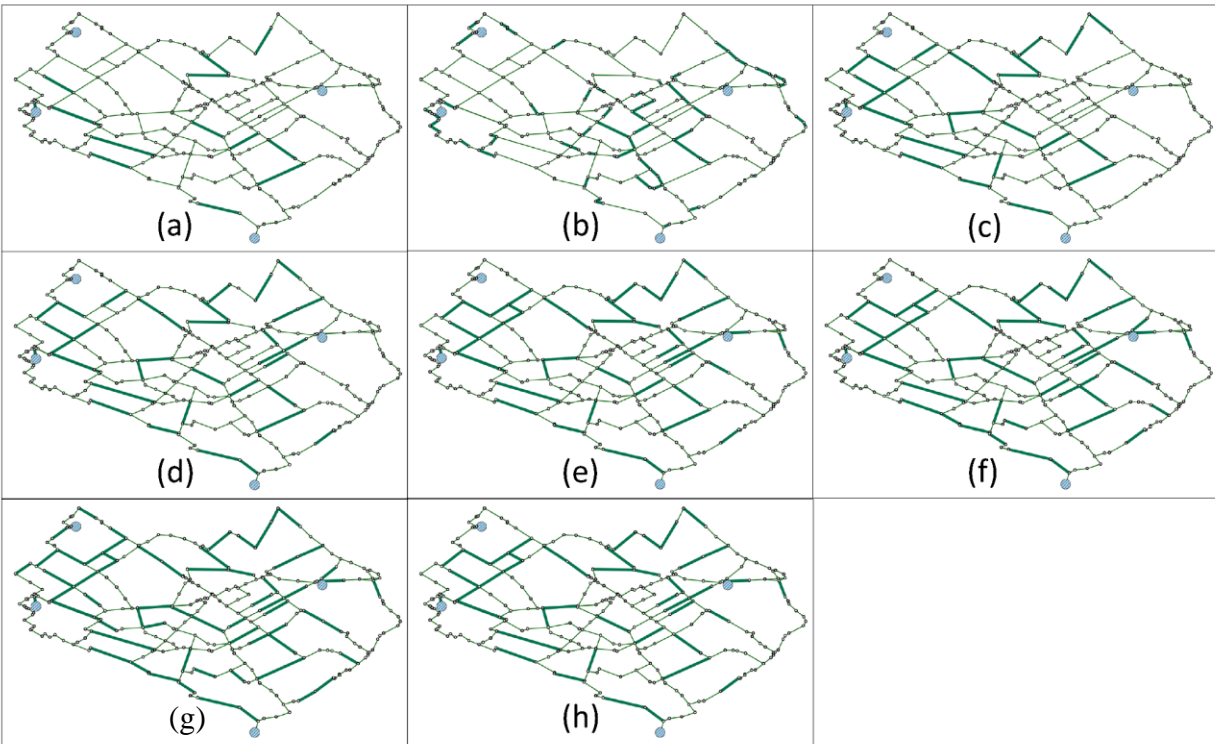
Figure 3-8. Critical pipes identified by simple length-based prioritization scheme for Modena network

Table 3-3. Results based on simple length-based prioritization scheme for Modena network

Percentage of total pipe length allowed for rehabilitation	Percentage of total pipe length actually rehabilitated	Expected SSI	Variance
Not more than 15	14.741	0.8290	0.0318
Not more than 20	19.417	0.8426	0.0288
Not more than 25	24.454	0.8455	0.0295
Not more than 30	29.599	0.8528	0.0281
Not more than 35	34.735	0.8702	0.0252
Not more than 40	39.516	0.8818	0.0246
Not more than 45	44.987	0.8902	0.0225
Not more than 50	49.964	0.9002	0.0202

3.4 Conclusions

An approach to identify critical pipes for resource-constrained seismic rehabilitation and to improve post-earthquake serviceability of a water pipe was created by integrating a genetic algorithm with a network-level seismic vulnerability assessment. This integration enables the identification of critical pipes, for distribution of rehabilitation resources at the system level. The application of the created approach was demonstrated using benchmark networks developed for testing algorithms dealing with formulating resilient designs of large water pipe networks. Furthermore, the results obtained from our proposed methodology was compared to the results obtained by using simple length prioritization scheme. Results demonstrated that the methodology

created in this study outperforms the simple prioritization scheme practiced by utilities. Additionally, the created approach was also validated by using identifying critical pipes for seismic rehabilitation in a water distribution network developed by the US EPA. These results were then compared with the latest methodology in literature. The comparison showed that our methodology identified more economical seismic rehabilitation policy compared to the most recent proposed approach in the literature when there are limitations about the length of pipes that can be rehabilitated. It is expected that the result of this study will help water utilities make informed decisions that will enhance post-earthquake serviceability of the water pipe networks.

CHAPTER 4

PROACTIVE SEISMIC REHABILITATION OF WATER PIPE NETWORKS SUBJECT

TO BUDGET CONSTRAINT USING SIMULATED ANNEALING

This chapter describes the simulated-annealing based methodology adopted to of identify critical pipes for proactive seismic of water pipe networks. The methodology can be divided into formulating optimization problem and solving the optimization problem. The definitions and solution methodology adopted accomplish these tasks are explained in following sections.

4.1 Pipe Network Definition

Pipe network is defined as a collection of pipes delivering water from a finite number of water sources to a finite number of demand nodes. The attributes of network are as follows:

- N is the number of nodes in the pipe network. A node may or may not have a water demand. Nodes with negative pressure are assumed non-functional (Markov et al. 1994; Shi 2006).

- N_p is the number of pipes in the pipe network.

- Pipe network is provided with finite number of water sources and water tanks. Constant water demand is used for this study.

4.2 Post-Earthquake Serviceability Indicator

System serviceability index (SSI) is used as an indicator to measure the serviceability after an earthquake event where SSI is defined as the ratio of water demand fulfilled after an earthquake to inherent demand of water pipe system (Shi 2006; Wang et al. 2010). If the water pressure at a demand node is above the threshold pressure, then the demand is supposed to be fulfilled at that node. Using these definitions, SSI is formulated as shown by Eq. (4-1).

$$SSI(x = \alpha) = \frac{\sum_{i=1}^{N} x_i^{\alpha} D_i}{\sum_{i=1}^{N} D_i} \tag{4-1}$$

Subject to

$$x_i^{\alpha} = 1 \; if \; P_i^{\alpha} \geq P_{threshold}$$

$$x_i^{\alpha} = 0 \; if \; P_i^{\alpha} < P_{threshold}$$

where N is the number of nodes in the network, D_i is the water demand at node i, P_i^{α} is the hydraulic pressure at node i for rehabilitation policy α, and $P_{threshold}$ is the minimum hydraulic pressure required at the node, imposed by the firefighting demand. In this study, a hydraulic pressure of 0.14 MPa (20 psi) was used as the $P_{threshold}$, as suggested by Trautman et al. (2013).

4.3 Problem Formulation

The problem is formulated as an optimization problem which aims to maximize the expected value of system serviceability index (*SSI*). Mathematical model of the optimization is represented by Eq. (4-2) and Eq. (4-3).

$$\max_{x \in X} E[SSI(x)] \tag{4-2}$$

Subject to

$$Cost(x) \leq C_{max} \tag{4-3}$$

where **X** represents the set of all possible rehabilitation policies, and each rehabilitation policy (x) represents the decision of the utilities to rehabilitate certain pipes, $Cost(x)$ represents cost of rehabilitation policy x, C_{max} represents maximum rehabilitation budget available to the utilities.

Evaluation of SSI involves determining the locations of seismic damages (leaks and breaks) in pipes. Occurrences of such damages are stochastic. Additionally, the nature of selecting pipes for

rehabilitation makes this optimization a combinatorial optimization. Stochastic objective function and combinatorial decision space makes optimization problem represented by Eq. (4-2) and Eq. (4-3) a stochastic combinatorial optimization. Furthermore, the objective function is non-convex and non-linear without any closed form representation.

4.4 System of coding

For this study, each rehabilitation policy, x, is a potential solution. Binary encoding is used to represent x. Hence, x has the same number of bits as the number of pipes in the water pipe network. There exists a one to one relationship between each bit in x and a pipe in the network. If a bit in x has a value of 1 then it means, the rehabilitation policy x suggests rehabilitating the pipe associated with that bit. If the bit has a value of 0, then the rehabilitation policy x suggests leaving the pipe associated with that bit unrehabilitated. For example, a potential rehabilitation policy for a network with 4 pipes could be [1001]. This string suggests rehabilitation of only the first and the last pipe of the network.

4.5 Integrated Simulated Annealing, Network-Level Seismic Vulnerability Assessment, and Monte Carlo Simulation

The lack of closed form representation of objective function and stochastic combinatorial nature of the optimization makes the problem really challenging. Hence, simulated annealing is adopted to solve the optimization represented by Eq. (4-2) and Eq. (4-3) as simulated annealing is effective in optimization of such complex, non-differentiable objective function. Simulated annealing is inspired by the process of solid annealing where the set of states of the solid is analogous to the set of potential solutions; energy is analogous to the objective function; and rate of cooling of solid is analogous to the temperature schedule in simulated annealing (Kirkpatrick et al. 1983). The algorithm uses metropolis criterion (Metropolis et al. 1953) to select or reject new solutions. At

the initial stages of simulated annealing, temperature is set at high value. At these stages, simulated annealing has high probability of accepting inferior solutions. Hence, simulated annealing is more exploratory when temperature is high. In contrast, at low temperatures, only the solution with higher fitness value than the current solution is accepted. Hence, at low temperature simulated annealing behaves as traditional hill-climbing algorithm. As such, temperature of simulated annealing is the indicator of the algorithm's probability of accepting inferior solutions. The rate of cooling determines the rate of transition of the algorithm from an exploratory algorithm to a traditional hill-climbing algorithm. The initial exploratory stage of the algorithm reduces chances of the algorithm being trapped in locally optimal values and increases the chances of identifying promising regions of decision space. The final hill climbing stage of the algorithm leads to fine tuning of the optimal value within the most promising region of decision space. Combination of initial temperature and the rate of cooling determines the convergence of algorithm to optimal solution in a finite amount of time. More information regarding initial temperature, rate of cooling, and stopping criteria can be found in Ingber (1993). Typically, sensitivity analysis is conducted to fix these parameters (Chen and Shahandashti 2009; Cunha and Sousa 1999). The simulated annealing algorithm integrated with network-level seismic vulnerability assessment of water pipe network adopted for this study is illustrated in Figure 4-1.
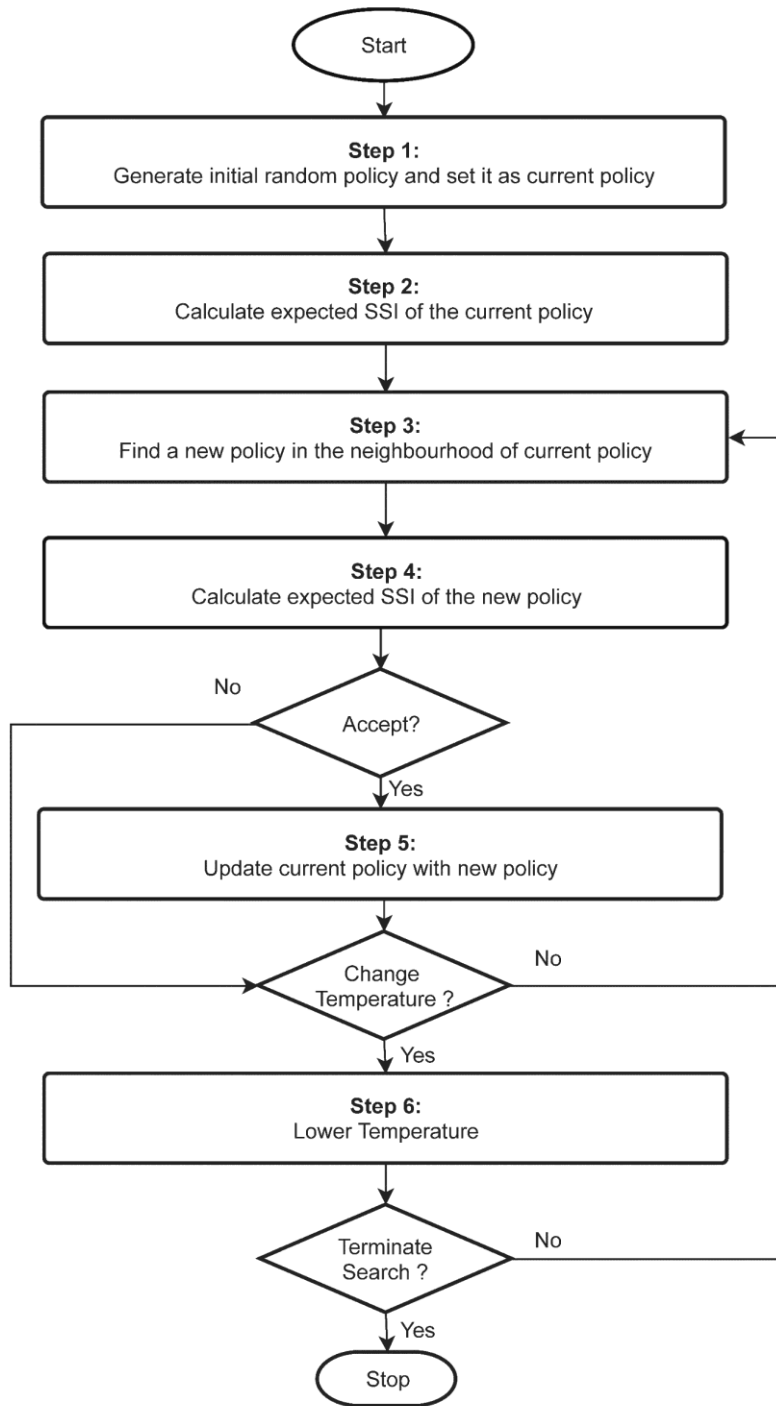
Figure 4-1. Simulated annealing integrated with network-level seismic vulnerability assessment

of water pipe network

4.6 Initialization of simulated annealing

Simulated annealing is initialized by randomly selecting a rehabilitation policy x. The cost of rehabilitation policy x *(i.e. Cost(x))* is calculated. There can be two cases; Case 1: $Cost(x) > C_{max}$ and Case 2: $Cost(x) \leq C_{max}$. For both the cases, we use a greedy heuristic (Wolsey and Nemhauser 1999) to eliminate the evaluation of infeasible or cheap policies. We choose to use this heuristic because greedy heuristic is known to give a good feasible solution (Wolsey and Nemhauser 1999). Hence, if the current rehabilitation policy x belongs to Case 1 i.e. if $Cost(x) > C_{max}$, we update x by removing the shortest rehabilitated pipe from the set of rehabilitated pipes. We continue this process till $Cost(x) > C_{max}$ is valid. However, if the current rehabilitation policy x initially belonged to Case 2 i.e. if $Cost(x) \leq C_{max}$, we update the current policy x by adding unrehabilitated pipes to the set of rehabilitated pipes. This addition of unrehabilitated pipes is continued till anymore addition leads to $Cost(x) > C_{max}$. At this stage, the greedy heuristic is terminated, and we obtain an updated rehabilitation policy x, which is always feasible. Subsequently, the simulated annealing is initialized with an initial temperature of 100 and the cooling rate of 2 at each decrement. Ten iterations were performed before each temperature decrement. These parameters of simulated annealing were finalized based on the sensitivity analysis.

4.7 Evaluation of objective function

Evaluation of objective function begins with the calculation of seismic pipe repair rate for each pipe in the network. The process of calculation of seismic pipe repair rate is illustrated in Figure 4-2.
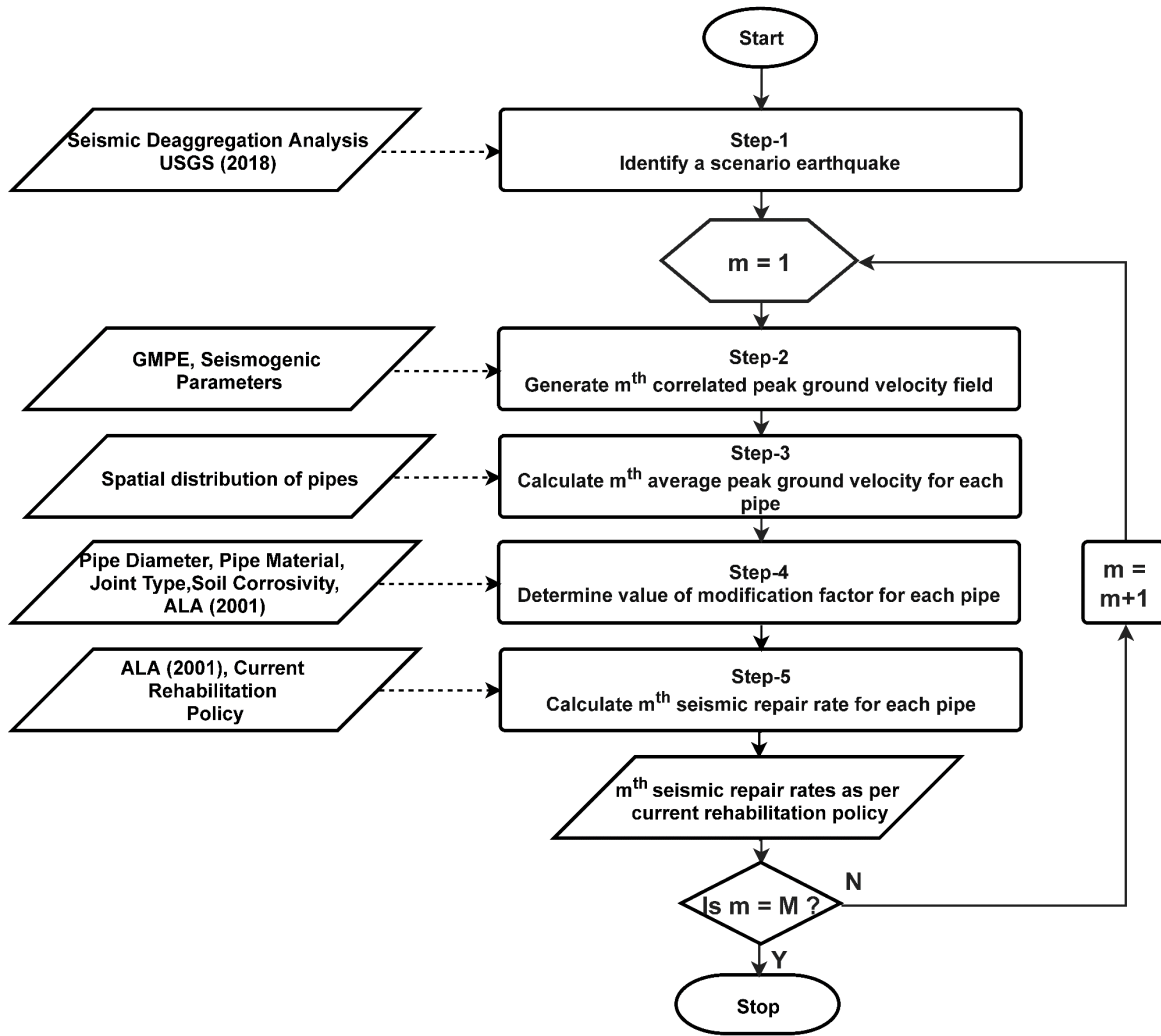
Figure 4-2. Seismic pipe repair rate calculation for current rehabilitation policy of simulated annealing

For the calculation of the seismic pipe repair rate, peak ground velocity fields were generated using the approach described in Chapter 3. Seismic pipe repair rates were then calculated using Eq. (4-4) based on ALA (2001),

$$RR_{m,k}^{x=\alpha} = K1 * 0.00187 * PGV_{m,k} * (1 - a_k^{x=\alpha}) \tag{4-4}$$

where $RR_{m,k}^{x=\alpha}$ is the seismic pipe repair rate of pipe k based on rehabilitation policy $x=\alpha$ and m^{th} peak ground velocity field, $K1$ is the modification factor which adjusts the repair rate based on pipe material, pipe diameter, pipe joint characteristics, and soil corrosivity. The values of $K1$ are tabulated in ALA (2001). $PGV_{m,k}$ (measured in inches/second) is the average peak ground velocity at the location of the pipe k due to the mth peak ground velocity field ; $a_k^{x=\alpha}$ is 0 if pipe is unrehabilitated based on policy $x=\alpha$, and $a_k^{x=\alpha}$ is 1 if pipe is rehabilitated based on policy $x=\alpha$. Setting $a_k^{x=\alpha}$ as 1 if pipe is rehabilitated based on policy $x=\alpha$ is equivalent to assuming that the rehabilitated pipe is not vulnerable to earthquakes anymore. One method to ensure this is to replace the critical pipes with earthquake resistant ductile iron pipes. These pipes have no record of any leaks and breaks in some major earthquakes in Japan where almost all other utilities and infrastructures were severely affected (Haddaway 2015). Therefore, for this study, the critical pipes are assumed to be replaced with earthquake resistant pipes during seismic rehabilitation of the network. As such, seismic pipe repair rate is calculated for each pipe in the network based on rehabilitation policy $x=\alpha$ for M different peak ground velocity field. Following this, objective function is evaluated using Eq. (4-5).

$$\max_{x \epsilon \mathbf{X}} E[SSI(x = \alpha)] = \frac{\sum_{m=1}^{M} \sum_{r=1}^{NMCS} SSI_r^m(x=\alpha)}{M*NMCS} \tag{4-5}$$

where $NMCS$ is the maximum number of Monte Carlo simulation runs adopted for evaluating each rehabilitation policy, $SSI_r^m(x = \alpha)$ is the system serviceability index calculated using Eq. (4-1) for r^{th} Monte Carlo run for the rehabilitation policy α, for m^{th} peak ground velocity field, M is the number of random peak ground velocity field generated for a single earthquake scenario.

4.8 Monte Carlo Simulation

Monte Carlo simulation is used to propagate component level seismic vulnerability of the pipes into the network to calculate expected serviceability of the network. Occurrence of earthquake-induced pipe leaks and breaks is modeled as Poisson process. The Monte Carlo simulation used in this study to accomplish this is shown in Figure 4-3.
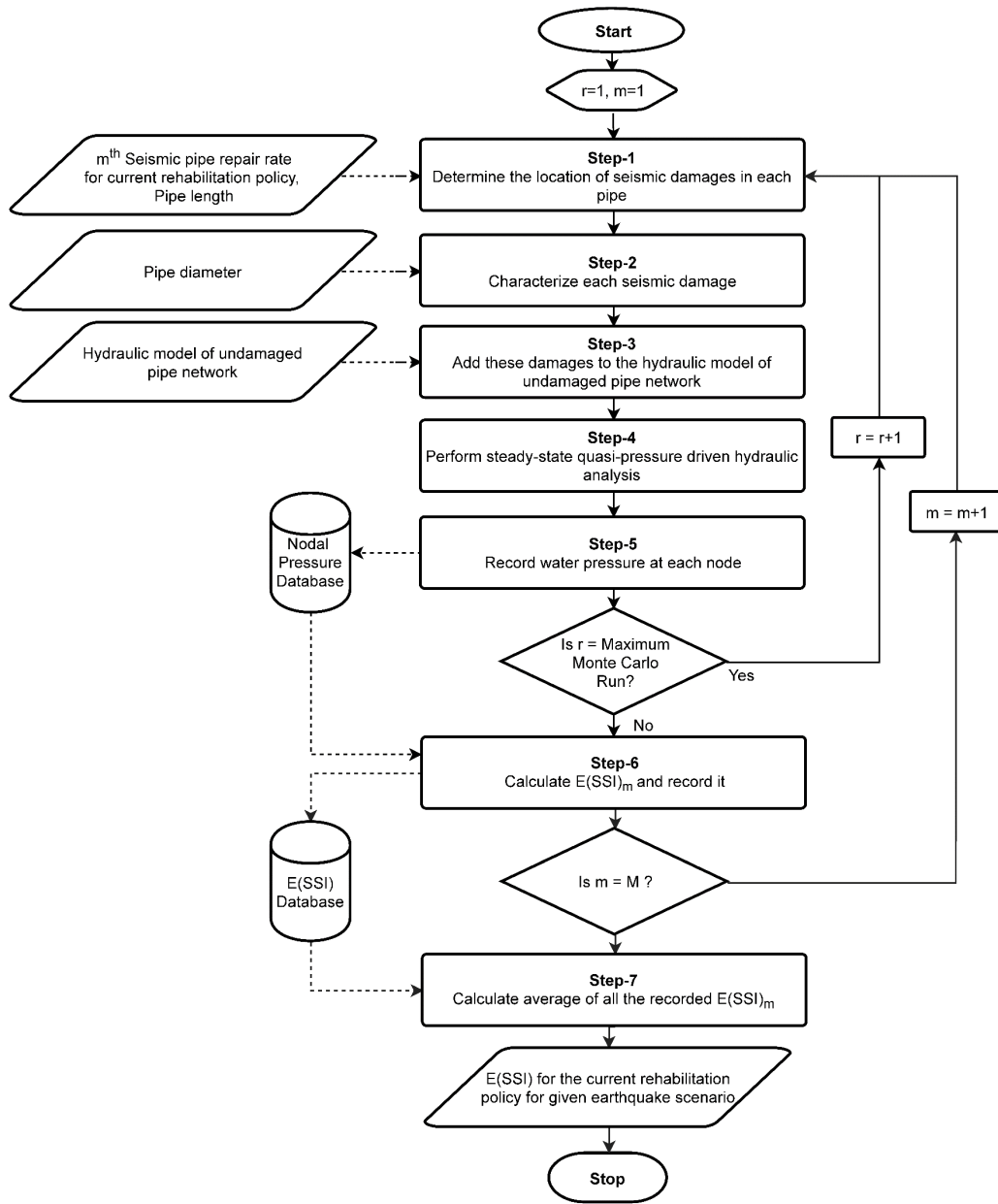
Figure 4-3. Monte Carlo simulation to evaluate the objective function of simulated annealing

Monte Carlo simulation adopted for this study generates *NMCS* scenarios of earthquake-induced

leaks and breaks in the water pipe network. For each scenario, the location of the ith leak or break

in a pipe p is determined by:

$$l_{p,i} = l_{p,i-1} - \frac{1}{RR_{m,p}^{x=\alpha}} * \ln(1 - U) \quad where \quad l_{p,0} = 0 \tag{4-6}$$

where $l_{p,i}$ is the distance of ith discontinuity (leak or break) in pipe p from its start node, $RR_{m,p}^{x=\alpha}$ is

the average seismic pipe repair rate calculated for the pipe p based on policy $x=\alpha$ for the mth peak

ground velocity field, and U is the uniformly distributed random number between 0 and 1. If the

location of the first leak or break lies within the length of the pipe p, i.e., if $l_{p,1}$ is less than the

length of pipe p, then a second random number is generated to classify it as either a leak or a break.

If the second random number generated is less than or equal to 0.8, the discontinuity at the location

$l_{p,1}$ is classified as a leak; otherwise, it is classified as a break (FEMA - Federal Emergency

Management Agency 2013; Shi 2006). Leaks are further classified, and the diameters of the leaks

are calculated based on Shi (2006). This process is repeated for higher values of i until the value

of $l_{p,i}$ exceeds the length of the pipe. The same process is repeated for other pipes in the network.

After all the leaks and breaks have been located and the diameters of all the leaks have been

determined for the current Monte Carlo run, they are integrated into the network hydraulic model

of the undamaged water pipe network. The hydraulic modeling of leaks and breaks proposed by

Shi (2006) is used for this process. The resulting hydraulic model is then analyzed, using a quasi-

pressure-driven steady-state hydraulic analysis, to determine the hydraulic pressure at each

node(P_i^{α}). This analysis is required because conventional demand-driven steady-state hydraulic

analysis assumes that the hydraulic demand at each node is always fulfilled, and that may not be a

valid assumption for water pipe networks damaged by an earthquake (Cheung et al. 2005; Ozger

and Mays 1994; Shi 2006). Hydraulic analysis, with the assumption that nodal water demand is not always fulfilled and that the system cannot have negative pressure in the nodes imitates the performance of actual networks after earthquakes (Shi 2006). Therefore, for this study, the quasi-pressure-driven analysis approach is adopted, and the following operations were performed for each run of the Monte Carlo simulation:

1) Hydraulic model with integrated leaks and breaks is analyzed.

2) Nodes with negative pressure are identified and removed from the network.

3) Step 1 and step 2 are repeated until there were no nodes with negative pressure.

Using this approach, the hydraulic pressure at each node (P_{ri}^{α}) is calculated and recorded for a predefined maximum number of Monte Carlo runs (NMCS) for the rehabilitation policy ($x=\alpha$). Then expected SSI of the rehabilitation policy ($x=\alpha$) is finally calculated using Eq. (4-1) and Eq. (4-5).

4.9 Progression of simulated annealing and its termination

After the evaluation of objective function for the first rehabilitation policy ($x = \alpha$) using Eq. (4-5), another rehabilitation policy ($x = \beta$) is identified by searching in the neighborhood of the first rehabilitation policy. This neighborhood search is accomplished by randomly mutating current rehabilitation policy ($x = \alpha$). In this study, twenty percent of binary string representing current rehabilitation policy ($x = \alpha$) is modified randomly. The cost of modified rehabilitation policy is calculated. Then, at this stage, we update the new policy ($x = \beta$) using greedy heuristic to eliminate infeasible and cheap rehabilitation policy. Subsequently, expected SSI of this new policy ($x = \beta$) is evaluated using Eq. (4-1) and Eq. (4-5). If the expected SSI of the new policy i.e. E(SSI($x = \beta$)) is greater than or equal to the expected SSI of the old policy i.e. E(SSI($x = \alpha$)), then the new policy

($x = \boldsymbol{\beta}$) is accepted and taken to the next iteration of simulated annealing. If the expected SSI of the new policy i.e. E(SSI($x = \boldsymbol{\beta}$)) is less than the expected SSI of the old policy i.e. E(SSI($x = \boldsymbol{\alpha}$), difference (δ) is calculated using Eq. (4-7) and r is calculated by using Eq. (4-8).

$$\boldsymbol{\delta} = \boldsymbol{e}^{\left(\frac{-(E(SSI(x=\alpha)-E(SSI(x=\beta)))}{t_c}\right)} \tag{4-7}$$

$$r = rand\ [0,1] \tag{4-8}$$

where t_c is the current temperature of the simulated annealing, *rand* [0,1] is a function to generate uniformly distributed random number between 0 and 1.

If $r < \delta$, then new rehabilitation policy ($x = \boldsymbol{\beta}$) replaces the old rehabilitation policy ($x = \boldsymbol{\alpha}$). If $r \geq \delta$, same old rehabilitation policy ($x = \boldsymbol{\alpha}$) is carried to next iteration of simulated annealing. This is known as Metropolis step. Temperature (t_c) is decreased at the selected cooling rate after allowing certain number of iterations at each temperature. Elitist strategy of saving the rehabilitation policy with highest expected SSI is adopted for this study to avoid the loss of good solutions. The simulated annealing progresses in this way by finding new rehabilitation policies, evaluating it, and replacing the old solution with the new using Metropolis step. The simulated annealing stops when the final temperature is reached. The rehabilitation policy with the maximum expected SSI up to this step in the algorithm is reported as the best rehabilitation policy for the given rehabilitation budget constraint.

4.10 Application

To demonstrate the application of the approach created in this study, we used a benchmark network called Modena network (Figure 4-4), from Center of Water Systems (2018) with 268 junctions, 317 pipes, and four reservoirs. The total length of the pipes of the entire network is 71806.11 m.

This network was created for resilience study of large dimensional water pipe network. For the calculation of seismic repair rate, pipes with diameter less than 300 mm (12 inches) were considered as Cast-Iron pipes with lead joints while pipes with diameter greater than 300 mm (12 inches) were considered as Ductile-Iron (DI) pipes with rubber gasketed joints.
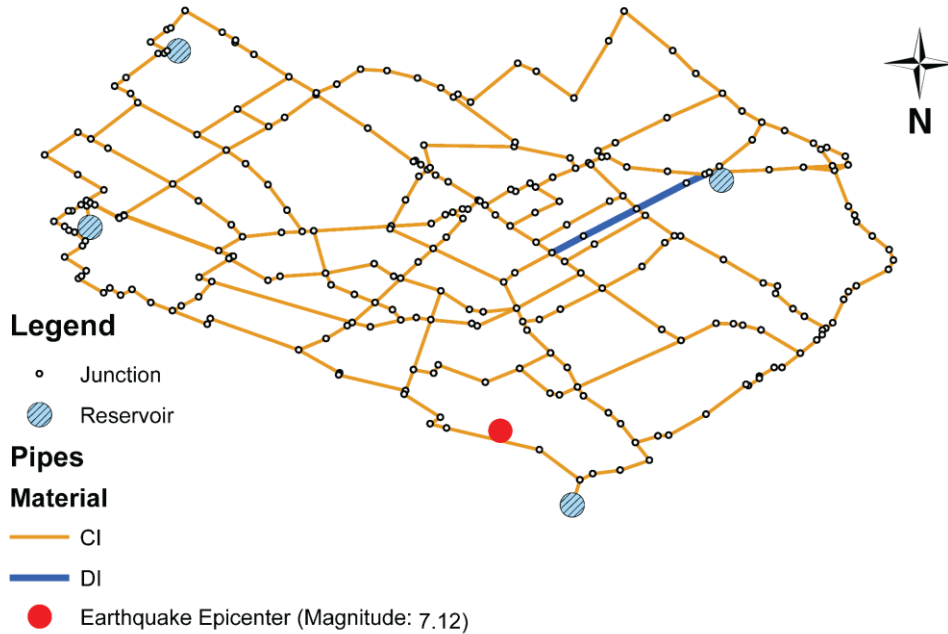
Figure 4-4. Modena Network

For selecting earthquake scenario, the location of the centroid of the network was assumed to be Pasadena, California (34.146267° N, 118.144040° W). A deaggreagation analysis was performed at 34.146267° N , 118.144040° W for 1.0 s spectral acceleration for the return period of 2475 years using USGS (2018). From the deaggregation result, an earthquake originating at Raymond fault, 3.25 km from the network's centroid, with a magnitude of 7.12 was identified as the earthquake with highest contribution ratio (13.84%). This earthquake was selected as the scenario earthquake. Peak ground velocity fields, as shown in Figure 4-5 and Figure 4-6, were generated using method described in Chapter 3. Subsequently, average peak ground peak ground velocities for each pipe

were calculated using method described in Chapter 3. These average peak ground velocities of all the pipes were then used to calculate expected SSI of the network using Eq. (4-5) for each rehabilitation policy.
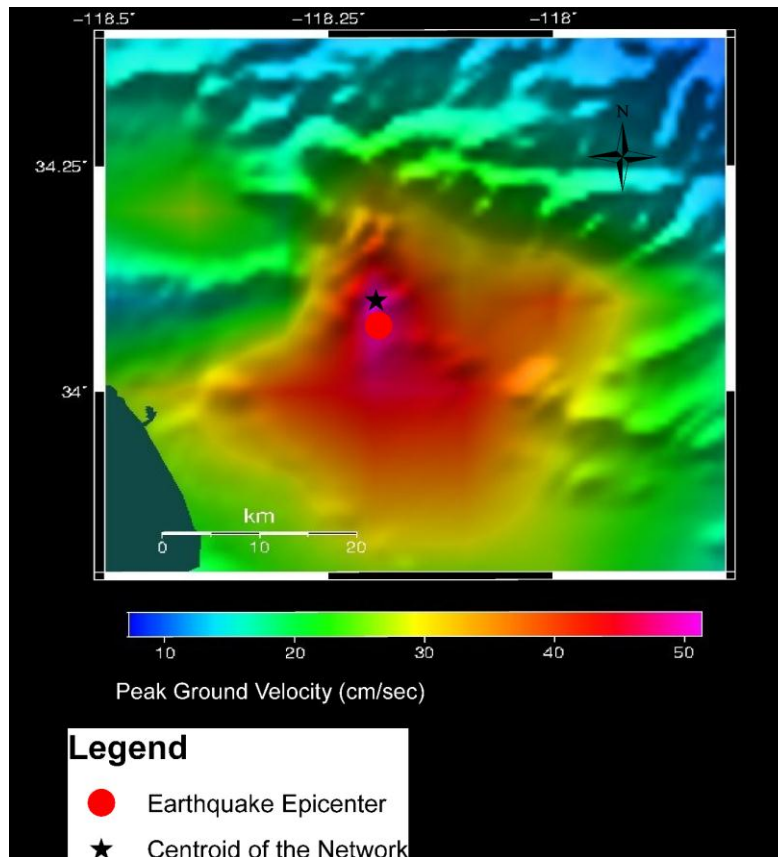
Figure 4-5. Peak ground velocity field due to the selected earthquake scenario without intra-event and inter-event residuals
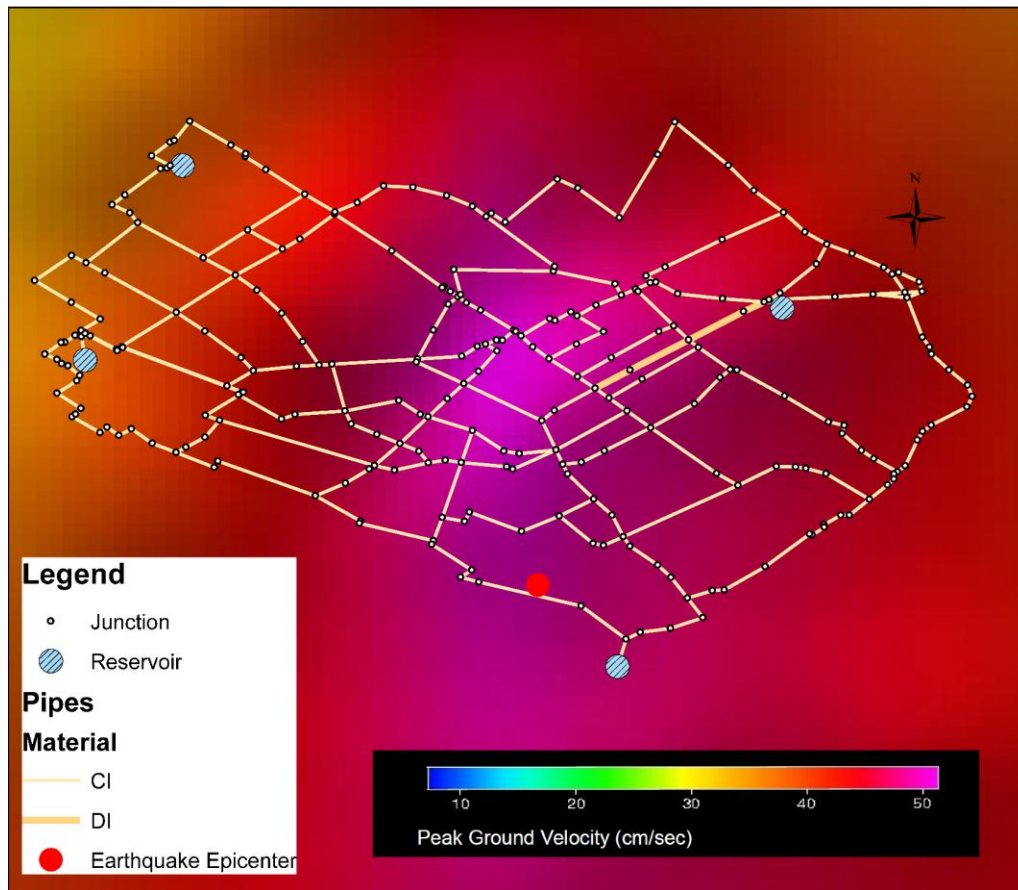
Figure 4-6. Peak ground velocity field due to the selected earthquake scenario without intra-event and inter-event residuals zoomed to the network's scale

To identify the adequate number of Monte Carlo runs, a convergence study was carried out (Figure 4-7). Modena network without any rehabilitation, subjected to the selected scenario earthquake, was chosen for the convergence study. No rehabilitation scenario was used because a network without any rehabilitation has the highest uncertainty compared to any rehabilitated scenarios. Hence, the number of Monte Carlo runs adequate to model the uncertainty for the unrehabilitated scenario would also be adequate for any rehabilitated scenarios. Convergence study, as shown in Figure 4-7 demonstrates that 3000 Monte Carlo runs is adequate. Hence, using 3000 Monte Carlo

runs, the expected SSI of the network, without any rehabilitation, was calculated as 0.785. Table

4-1 shows the parameters of the simulated annealing used.
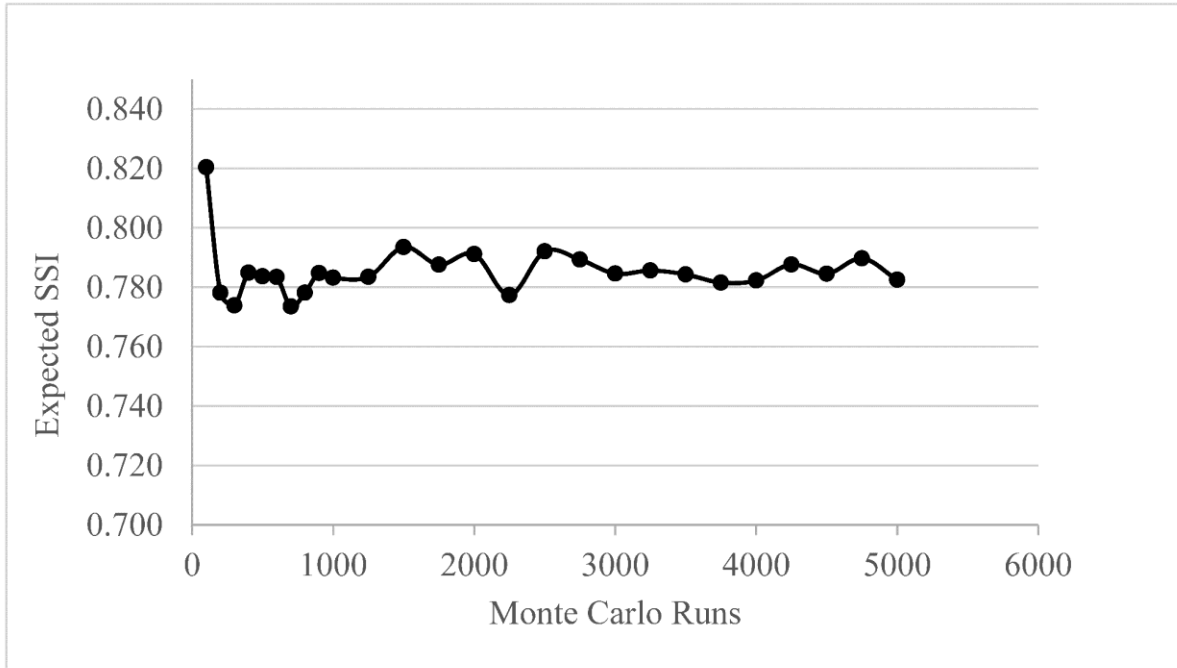
Figure 4-7. Convergence study to identify adequate Monte Carlo runs for the Modena **network**

Table 4-1. Simulated annealing parameters

Parameters	Value
Initial Temp	100
Final Temp	1
Cooling Rate	2
Iterations per Temperature	10
Maximum Monte Carlo Runs	3000
Total Iterations	500

The cost data used for the rehabilitation is summarized in Table 4-2. The material costs and bare costs for installing ductile iron pipes manufactured in United States were obtained from RS Means (2017). The backfill cost was obtained from JM Eagle (2017). They were added to get the total cost for installing ductile pipes manufactured in United States. Then, the cost of installing earthquake resistant Japanese ductile iron pipe were obtained by adjusting the price of US manufactured pipe. The adjustment was based on the fact that the earthquake resistant Japanese ductile iron pipe can be three times the price of US manufactured ductile iron pipes (Haddaway 2015). The information regarding the earthquake resistant pipes' readily available diameters was obtained via correspondence with one of the major manufacturers of the pipes to formulate a practical rehabilitation policy.

Table 4-2. Rehabilitation costs adopted for this study

	US manufactured ductile iron pipe				Earthquake resistant Japanese ductile iron pipe		
Pipe diameter (mm)	Material cost [a] (USD)	Bare cost without backfill cost[a] (USD)	Backfill cost [b] (USD)	Total cost with backfill cost (USD)	Bare cost without backfill cost [c] (USD)	Total cost with backfill cost (USD)	Normalized cost in terms of 101.6 mm diameter pipe
101.6	30.50	42.58	4.49	47.07	103.58	108.07	1.00
152.4	26.50	41.57	5.15	46.72	94.57	99.72	0.92

203.2	44.50	62.62	5.83	68.45	151.62	157.45	1.46
254.0	58.50	79.61	6.50	86.11	196.61	203.11	1.88
304.8	79.00	101.94	7.20	109.14	259.94	267.14	2.47
355.6	93.00	117.16	7.91	125.07	303.16	311.07	2.88
406.4	94.50	127.50	8.63	136.13	316.50	325.13	3.01
457.2	126.00	160.80	9.37	170.17	412.80	422.17	3.91
508.0	127.00	169.10	10.12	179.22	423.10	433.22	4.01
609.6	141.00	192.25	11.66	203.91	474.25	485.91	4.50

[a] These costs are based on the RS Means (2017) for class 50 water piping with 5.4864 m (18 ft.) length.

[b] These costs are based on JM Eagle (2017). Backfill is assumed to be 30.48 cm (1 ft.) above the top of the pipe, the backfill cost is assumed to be $0.015 per kg and the density of the backfill is assumed to be 2162.49 kg/m^3 (135 lb/ft^3).

[c] These costs assume that material cost of Kubota company manufactured earthquake resistant DI pipes is three times the cost of DI pipes manufactured in US based on Haddaway (2015)

Using the created approach and the normalized cost vector (last column of Table 4-2), rehabilitation policies were identified for different rehabilitation budget constraints for the Modena network. The results for such policies are shown in Table 4-3 while critical pipes identified corresponding to each of these policies are highlighted by thick green lines in Figure 4-8. The progression of simulated annealing is shown in Figure 4-9.

Table 4-3. Results of implementing the proposed methodology to the Modena network for

different rehabilitation budget constraint

Policy ID [a]	Rehabilitation cost upper bound (USD)	Actual cost of rehabilitation (USD)	Expected SSI	Variance of SSI	Solution Time [b] (Hrs.)
$S_{2.5}$	2.5 Million	2,499,331.50	0.89527	0.01959	295.53
$S_{5.0}$	5.0 Million	4,999,709.50	0.91035	0.01557	295.09
$S_{7.5}$	7.5 Million	7,495,438.50	0.92534	0.01120	287.29
$S_{10.0}$	10.0 Million	9,998,185.00	0.93876	0.00830	283.58
$S_{12.5}$	12.5 Million	12,463,533.00	0.95095	0.00761	284.05

[a]S_k means policy identified by our simulated annealing-based approach constrained such that

seismic rehabilitation cost cannot exceed k million USD.

[b]Solution time reported is for a workstation with Intel(R) Xeon(R) CPU E3-1240 v5 @3.50GHz

processor and 16.0 GB of RAM running Windows 7 Enterprise operating system.
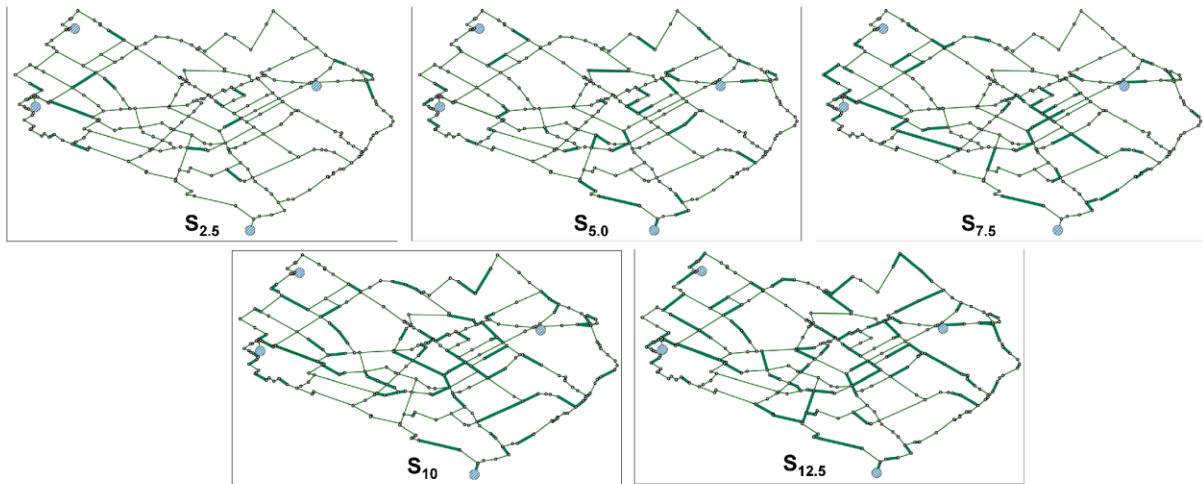
Figure 4-8. Critical pipes identified by our SA based approach for the Modena network
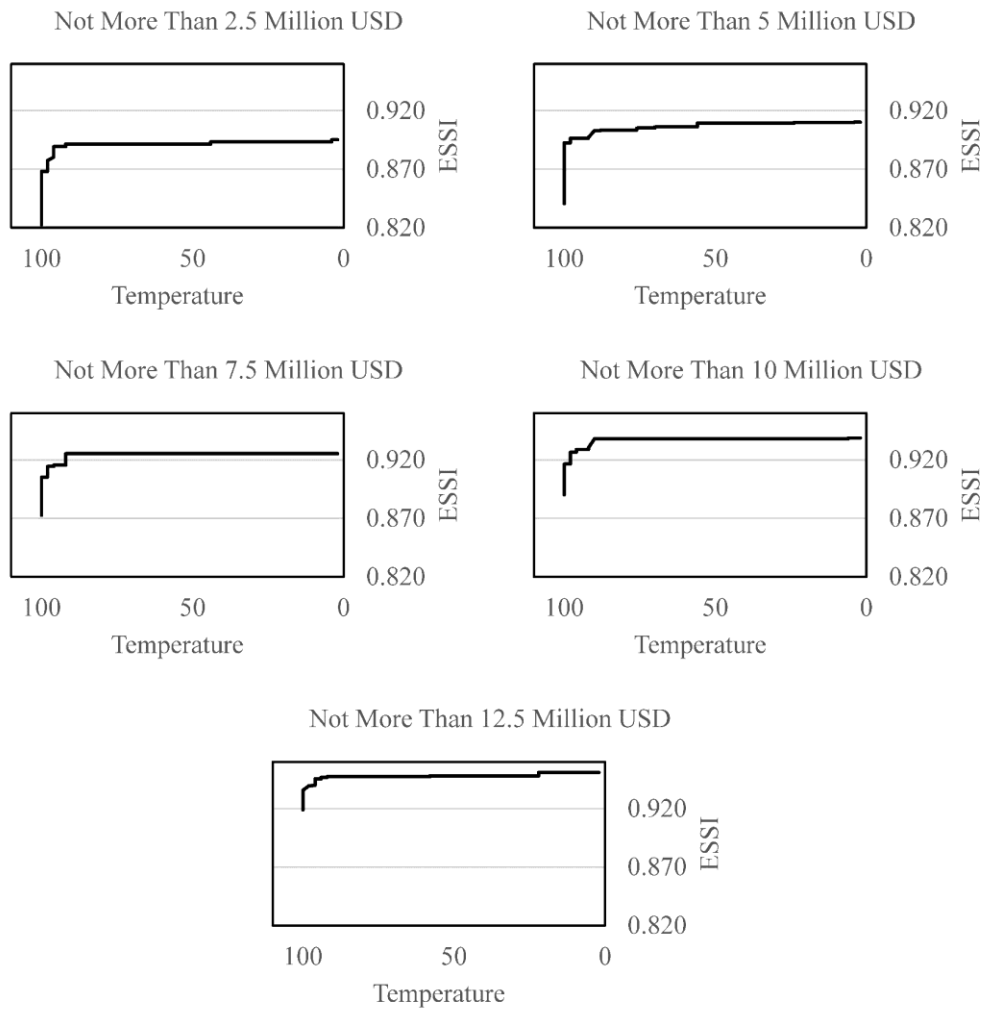
Figure 4-9. Progression of simulated annealing for different rehabilitation budget constraints for

the Modena network

4.11 Validation

For the first step in validation, rehabilitation policies were generated using simple length-based heuristic. Simple length-based heuristic is represented by L_k, where L_k refers to a length-based rehabilitation heuristic which prioritizes rehabilitating longer pipes such that cost of rehabilitation does not exceed k million USD. This length-based heuristic is similar to the greedy heuristic that we used to eliminate infeasible and cheap solutions in our SA-based approach. Hence, in this

heuristic, we try to rehabilitate the longest unrehabilitated pipe. We keep on doing this until the cost of rehabilitation is less than the cost constraint. During this process, there will be a stage when rehabilitating the longest unrehabilitated pipe will cause the cost constraint to be exceeded. When this happens, we then try to rehabilitate second longest pipe. If rehabilitating second pipe also leads to infeasible solution, third pipe is checked. This is continued till we cannot add rehabilitate even the shortest unrehabilitated pipes in the network. When this happens, the heuristic is stopped, and the resulting rehabilitation policy is analyzed. This heuristic was used to create 5 rehabilitation policies for cost constraints equal to that of SA based approach (in Table 4-3). These length-based policies were then analyzed. Figure 4-10 shows the pipes selected based on 5 policies identified by length-based heuristic. Results obtained for these cases are tabulated in Table 4-4. We selected this length-based heuristic to demonstrate that rehabilitating few long pipes in the network is less economical when compared to rehabilitating pipes identified by considering seismic vulnerability of network and network level distribution of rehabilitation resources. The comparison of the expected SSI of the policies identified by our SA based approach and length-based heuristic is done in Figure 4-11. It can be clearly seen from Figure 4-11 that, for the given network and the simulated earthquake, policies identified by our SA-based approach clearly gives significantly higher expected SSI when compared to the policies identified by the length-based heuristic.
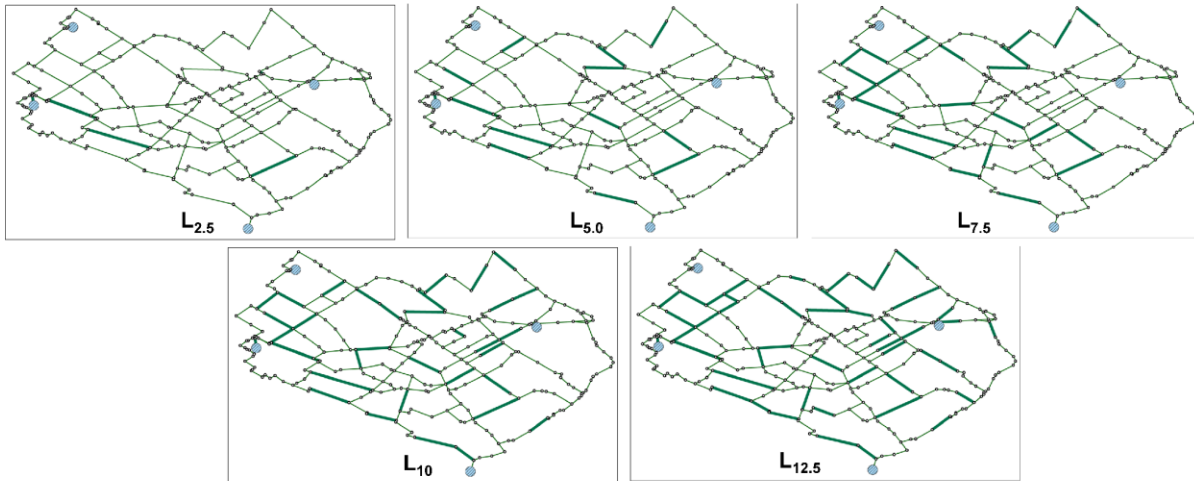
Figure 4-10. Critical pipes selected based on length-based rehabilitation heuristic

Table 4-4. Results for length-based rehabilitation heuristic prioritizing longer pipes for Modena network

Policy ID	Rehabilitation cost upper bound (USD)	Actual cost of rehabilitation (USD)	Expected SSI	Variance of SSI
$L_{2.5}$	2.5 Million	2,499,880.00	0.81604	0.03295
$L_{5.0}$	5.0 Million	4,999,680.50	0.84275	0.02833
$L_{7.5}$	7.5 Million	7,499,982.00	0.86752	0.02506
$L_{10.0}$	10.0 Million	9,998,892.00	0.88928	0.02084
$L_{12.5}$	12.5 Million	12,499,842.00	0.90582	0.01928

[a] L_k means length-based rehabilitation heuristic which prioritizes rehabilitating longer pipes such that cost of rehabilitation does not exceed k million USD
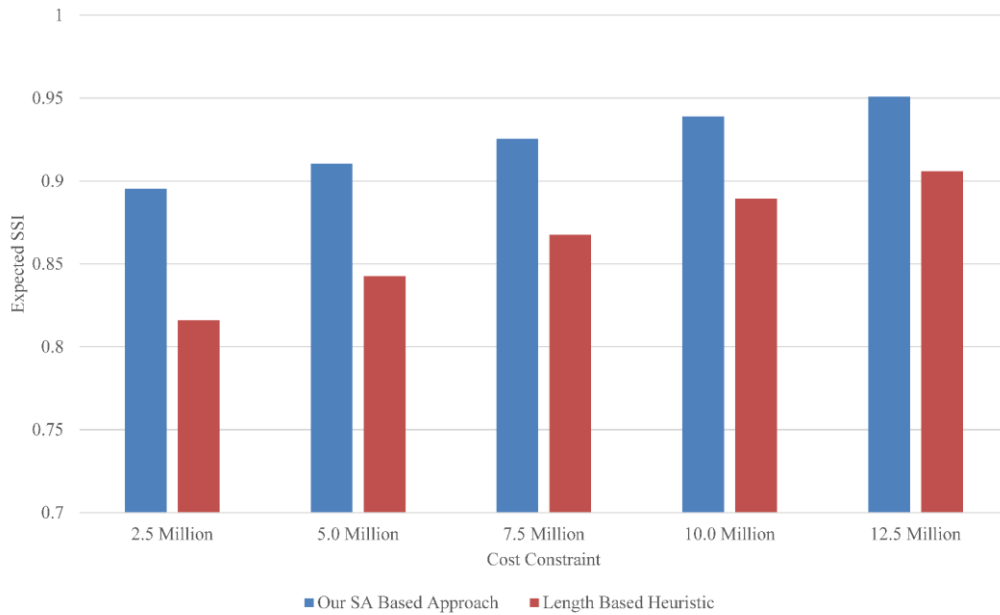
Figure 4-11. Comparison between expected SSIs of the policies identified by our SA based approach and length-based heuristic with the same cost constraint for the Modena network

For the next step in validation, the policies identified by our simulated annealing-based approach was compared to the rehabilitation policy suggested by Wang et al. (2010). Wang et al. (2010) uses EPANET example network (Figure 4-12) as the test-bed for implementing their methodology. The EPANET example network was developed by the US Environmental Protection Agency (US EPA) for testing models involving hydraulic simulation. The network is composed of 117 pipes and 92 junctions. A river and a lake supply water to the network while 3 tanks are provided within the network for storage. For this study, the water demand and material assignment of each pipe is based on Wang et. al. (2010). Hence, the pipes with diameters less than 24 inches are assumed as cast iron pipes with brittle joints while pipes with diameters 24 inches and above are assumed as steel pipes with welded joints. Setting the assignment of water demand and pipe materials as per Wang et al. (2010) facilitates comparing the results obtained using our methodology to the results obtained by Wang et. al. (2010). Furthermore, we had to use a uniform peak ground velocity of 50

cm/sec for this case because Wang et al. (2010) use this uniform peak ground velocity field for their analysis. Convergence study was conducted for the unrehabilitated EPANET network as well (Figure 4-13). The study indicated that 3000 Monte Carlo runs were adequate for this case as well. Hence, Table 4-1 and Table 4-2 were used to configure the SA based approach to identify critical pipes for this network as well. SA based approach configured as such was then used to identify the critical pipes for different rehabilitation budget constraints for the EPANET network. The details of the policies identified are shown in Table 4-5 while critical pipes identified corresponding to each of these policies are highlighted by thick green lines in Figure 4-14.
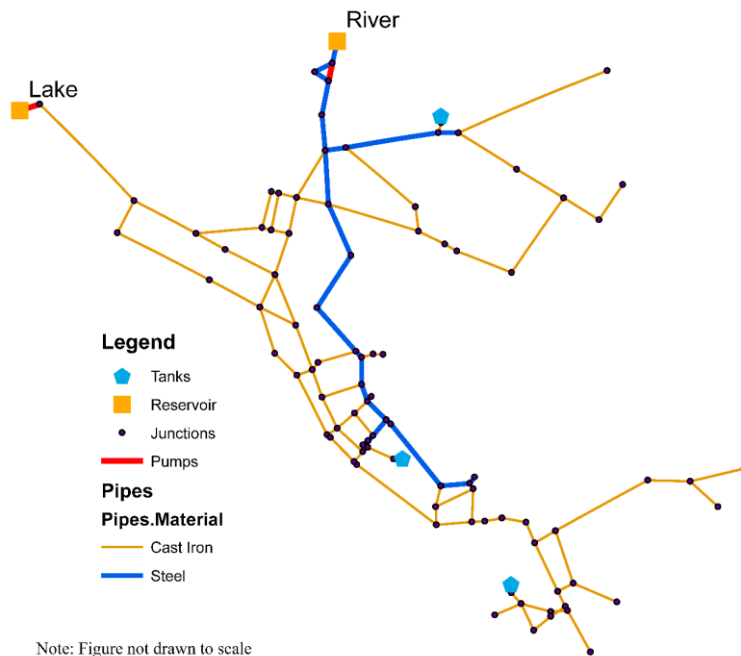
Figure 4-12. EPANET example network
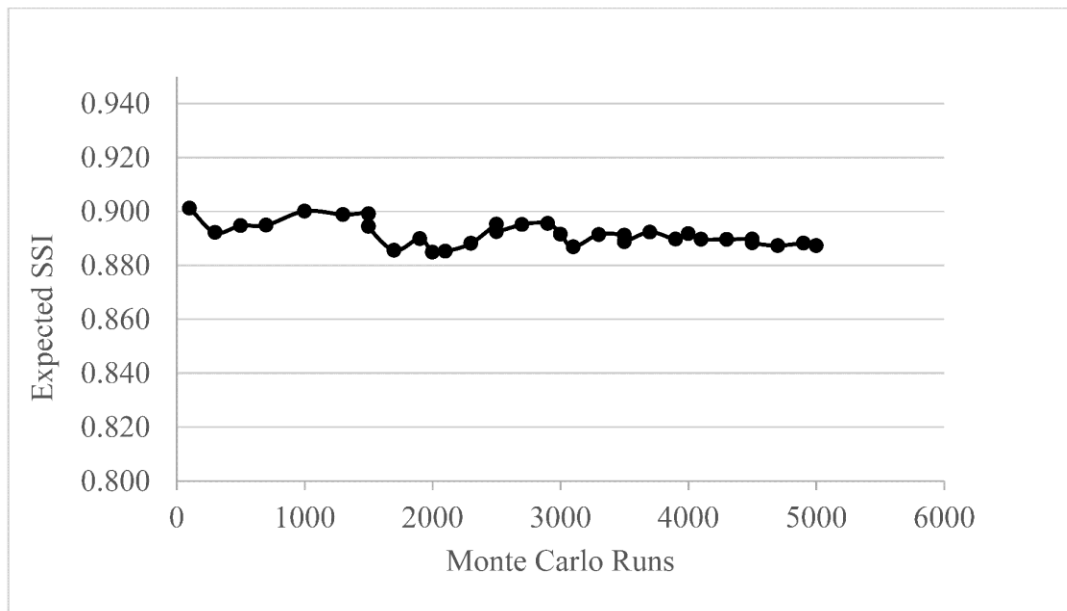
Figure 4-13. Convergence study to identify adequate Monte Carlo runs for the EPANET network

Table 4-5. Results of implementing our SA based approach to the EPANET network for different rehabilitation budget constraint

Policy ID [a]	Rehabilitation cost upper bound (USD)	Actual cost of rehabilitation (USD)	Expected SSI	Variance of SSI	Solution Time[b] (Hrs.)
S_{10}	10 Million	9,995,563.00	0.92675	0.03179	236.90
S_{15}	15 Million	14,878,407.00	0.93511	0.03200	238.55
S_{20}	20 Million	18,234,756.00	0.94798	0.02645	240.68
S_{25}	25 Million	23,619,262.00	0.95630	0.01708	236.68
S_{30}	30 Million	29,401,872.00	0.95821	0.01656	233.84

[a]S$_k$ means policy identified by our simulated annealing-based approach constrained such that seismic rehabilitation cost cannot exceed *k* million USD.

[b]Solution time reported is for a workstation with Intel(R) Xeon(R) CPU E3-1240 v5 @3.50GHz processor and 16.0 GB of RAM running Windows 7 Enterprise operating system.
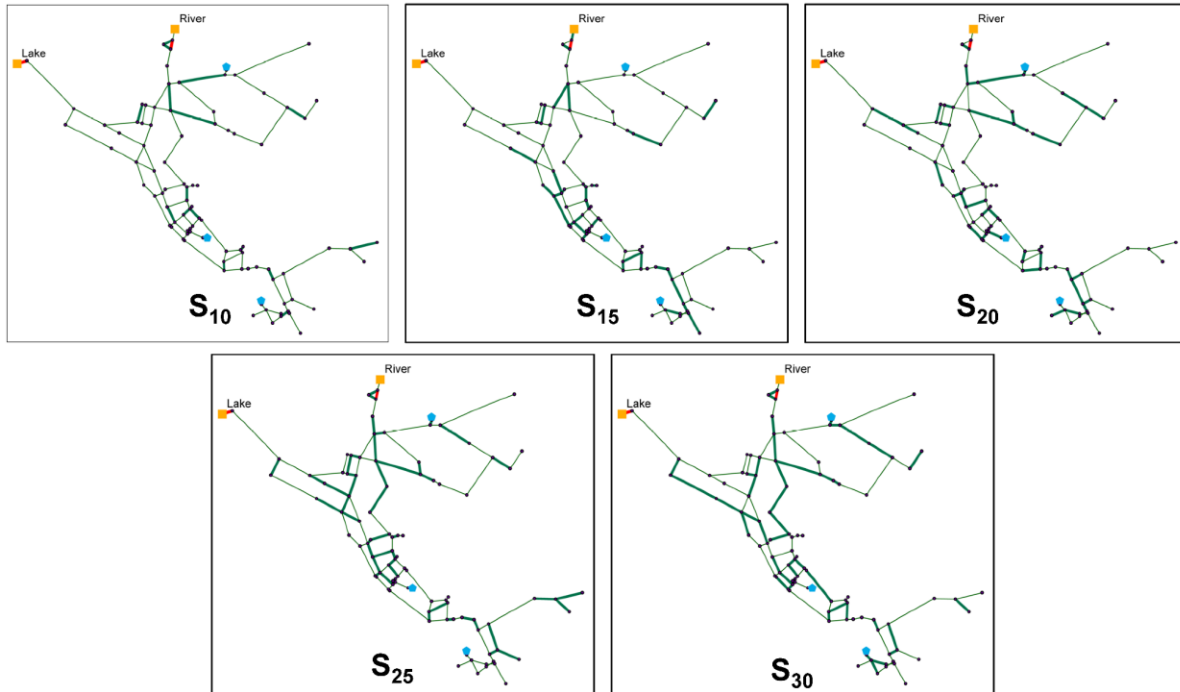
Note: Figure not drawn to scale

Figure 4-14. Critical pipes identified by our SA based approach for the EPANET network

For validation, these policies (From Table 4-5), were compared to the rehabilitation policy identified by Wang et. al. (2010). The pipes recommended for rehabilitation by Wang et al. (2010) are highlighted by thick red lines in Figure 4-15. The network, with these pipes rehabilitated, was analyzed, and the expected SSI was calculated for this case. Upon comparison of those results with the results of our approach (in Figure 4-16), it can be observed that policy identified by our approach for constraints of 20 million USD, 25 million USD, and 30 million USD have higher

SSI. However, these policies cost substantially less than Wang et al. (2010)'s policy, which costs nearly 60 million USD. This shows that, compared to Wang et al. (2010)'s approach, our approach was able to identify much more economical seismic rehabilitation policy for this test network against the simulated earthquake. However, a more general conclusion requires analysis of observations from more examples.

Note: Figure not drawn to scale
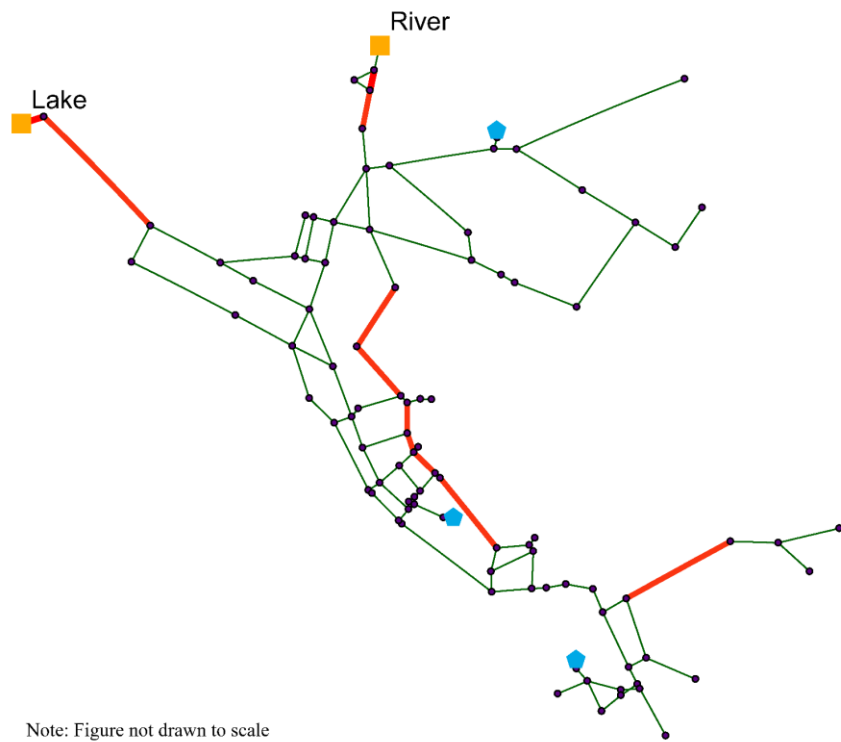
Figure 4-15. Critical pipes based on rehabilitation policy suggested by Wang et al. (2010) for the
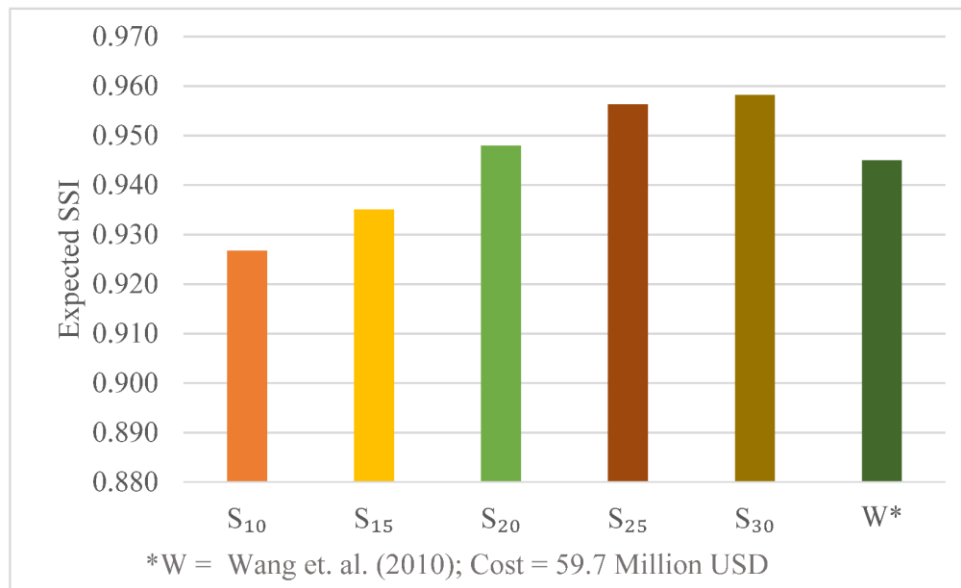
EPANET network

Figure 4-16. Comparison of expected SSI of policies identified by our SA based approach and rehabilitation policy identified by Wang et. al. (2010) for the EPANET network

4.12 Conclusions

Although many researchers propose approaches for seismic vulnerability assessment for the water pipe networks, approaches to identify critical pipes for seismic rehabilitation of water pipes are rare. However, even these rare approaches are based on some simple prioritization techniques or ignore the correlation between the effect of pipes' damages on the network serviceability. As such, there was a need of an approach to identify critical pipes for pro-active seismic rehabilitation of water pipe networks that is based on comprehensive seismic vulnerability assessment; that considers spatial correlation between seismic intensities; that considers limited rehabilitation budget; and does not ignore the correlation between the effect of pipes' damages on the network serviceability. To address this, a simulated annealing-based optimization is developed and integrated with network-level seismic vulnerability assessment of water pipe network to maximize its post-earthquake serviceability by considering network-level distribution of limited

rehabilitation resources. The developed approach is used to identify critical pipes for seismic rehabilitation of two benchmark networks. The results thus obtained were compared to the rehabilitation policy suggested by a simple length-based heuristic and the policy suggested by a latest methodology in literature. The comparison showed that our approach was able to identify more economical rehabilitation policy as compared to the simple length-based rehabilitation heuristic and the latest methodology in literature. The developed approach adds to the existing literature, a new method of considering network level distribution of limited rehabilitation resources for the seismic rehabilitation of water pipe networks. Moreover, the developed approach can be used by the water utility managers to formulate economical seismic rehabilitation policy for their water pipe networks when rehabilitation budget is constrained.

CHAPTER 5

**RESILIENCE METRICS AND PROACTIVE SEISMIC OPTIMIZATION OF WATER
PIPE NETWORKS**

This chapter describes the methodologies adopted in this study to evaluate the performance of a wide range of resilience metrics and their suitability as objective function for optimization of seismic rehabilitation of water pipe networks. Water pipe networks are often subjected to devastating natural disasters such as earthquakes. To ensure reliability of these networks against such earthquakes, seismic resilience of the networks must be analyzed and subsequently enhanced via a combination of proactive and reactive rehabilitation. Calculating resilience of a water pipe network presents many challenges. One of these is to identify a proper metric of resilience. Klise et al. (2015) reports that currently there is lack of a satisfactory resilience metric for water supply systems.

Currently available resilience metrics can be divided broadly into two categories: qualitative and systems-modeling based metrics. Qualitative resilience metrics are in the form of qualitative ranking, scorecard, and indexes (Fiksel et al. 2014; Fisher et al. 2010). Even though these metrics are flexible enough to combine information from distinct fields and invite collaboration of diverse stakeholders, these metrics are highly subjective and cannot capture the dynamic linkages and feedback loop inherent in water supply systems (Klise et al. 2015). In contrast, systems-modeling based metrics are in the form of mathematical models which are designed to simulate the actual behavior of water supply systems subjected to damages. These metrics can effectively identify dynamic interactions between the components of water supply system and help examine the linkage between them, especially when these systems are damaged by some catastrophic events.

These systems-modeling based metrics can be further divided into two sub-categories: topological based and hydraulics based.

Topological metrics are based on graph theory. To calculate resilience of water supply system using these metrics, the water supply systems are modeled as graphs i.e. $G(V, E)$ where V is the set of nodes or vertices in the network and E is the set of pipes or arc in the network. Commonly, the network is modeled as bidirectional graphs. Hence, each pipe is modeled as two directed arcs. Such metrics offer a simplified approach of modeling water supply systems since they simply the analysis by ignoring the hydraulics and physics of water flow through the water supply system. Hydraulics based metrics such as Available Demand Fraction (Ozger and Mays 1994), System Serviceability Index (Shi 2006; Wang et al. 2010), and Entropy Based Reliability (Awumah et al. 1991) are based on physics that govern the flow of water in a water pipe systems. Hence, hydraulics-based metrics are better suited for a more rigorous study. However, these hydraulic equations tend to make the model more complex and data hungry.

A lot of researchers have used the above described metrics to study the resilience of water pipe networks. First group of studies is based on topological metrics. Jacobs and Goulter (1988, 1999) showed network represented by regular graphs are least vulnerable. A regular graph is a graph where each vertex has the same number of neighbors; i.e. every vertex has the same degree or valency. Ostfeld (2005) proposed a methodology to identify operational and backup digraph that yielded one-level system redundancy. Fragiadakis et. al. (2014) used fragility formulation by ALA (2001) and Djikstra's shortest path algorithm to assess reliability of water pipes networks subjected to earthquakes. Another group of studies used hydraulic based metrics. Shi (2006) and Wang et al. (2010) used System Serviceability Index to measure seismic resilience of water pipe networks and thus studied seismic response of water supply systems.

As such, a variety of metrics based on network topology (e.g. redundancy, average path length), hydraulics (e.g. Available Demand Fraction), and entropy (e.g. Entropy Based Resilience) could be used to analyze the seismic resilience of water pipe networks. Performance of seismic optimization algorithms for water pipe networks depends on the selection of these resilience metrics. Even though a few rare research has been done using some of these metrics in optimization of water pipe networks (Pudasaini et al. 2017; Pudasaini and Shahandashti 2018; Shahandashti and Pudasaini 2019), there is no research that studies the tradeoff between computational economy and solution quality when these metrics are used for resource constrained seismic optimization of water pipe networks. Hence, the objective of this study is to:

- analyze the performance of a variety of resilience metrics in the resource-constrained seismic rehabilitation optimization of the water pipe networks
- identify the trade-off between solution economy and solution quality associated with each metrics.

The methodology adopted to study the performance of various topological metrics as the objective function for maximizing seismic resilience of water pipe networks was executed in the steps which are explained in the following sections.

5.1 Modeling of water pipe network as a graph

Water pipe network was modeled as a bi-directional graph $G(V, E)$ where V is the set of vertices of the graph and E is the set of edges of the graph. Each junction of the water pipe was assigned to vertex set V. For each pipe, two directed edges were defined where one edge was directed from the start node of the pipe to the end node while the other edge was directed from the end node to the start node. This is illustrated in Figure 5-1.

$$G(V, E)$$

$$V = \{1, 2, 3, 4\}$$
$$E = \{(1,2), (2,1), (2,4), (4,2), (2,3),$$
$$(3,2), (2,5), (5,2), (3,5), (5,3),$$
$$(4,5), (5,4)\}$$
$$Source = \{1\}, Demand = \{4, 5\}$$

● Source

○ Junction

⚲ Service Junction
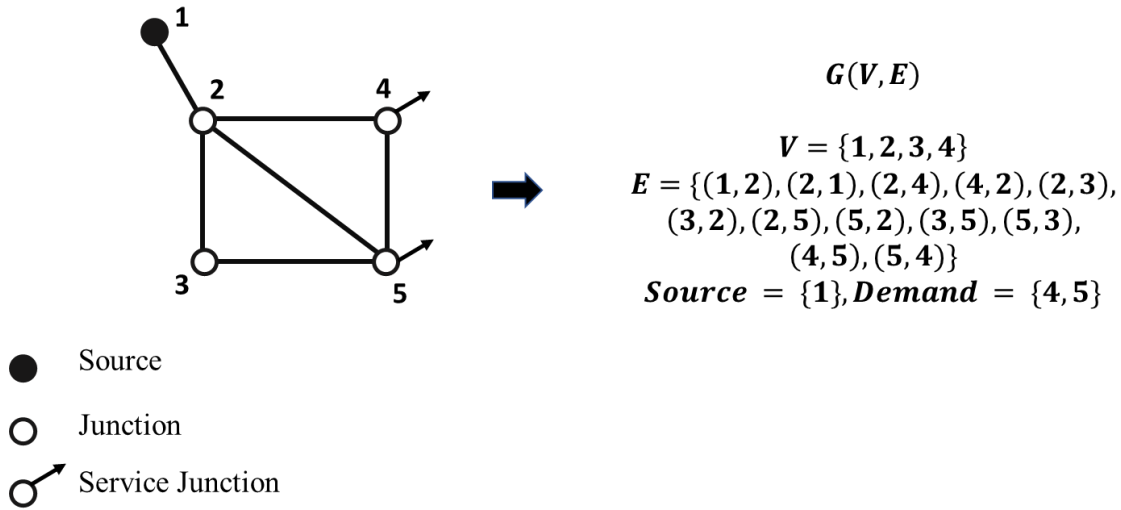
Figure 5-1. Modeling of water pipe network as a graph

5.2 Evaluation of Seismic Resilience Metrics

Various topological metrics defined in the literature of graph theory (Bondy and Murty 2008; Diestel 2000) and social network analysis (Wasserman and Faust 1994) were used in this study to quantify seismic resilience of the water pipe network. Each of them is defined below with its formulation:

5.2.1 Link Density (ρ_{Link}):

It is defined as the fraction between the total and the maximal number of edges in the graph. It is calculated for a graph using Eq. (5-1). For a water pipe network, link density indicates how linked or sparse the water pipe network really is (Haegele 2016; Paez and Filion 2017; Yazdani et al. 2011).

$$\rho_{Link} = \frac{2|E|}{|V|(|V|-1)} \qquad \textbf{(5-1)}$$

5.2.2 Average Node Degree ($\bar{d}$):

Average node degree is the measure of the average number of edges incident to a node in the graph. It is calculated using Eq. (5-2). For water pipe network, if most of the nodes have degree close to average node-degree, then it indicates equalized distribution of flow and pressure under varying demands in the network (Haegele 2016; Paez and Filion 2017; Yazdani et al. 2011).

$$\bar{d} = \frac{2|E|}{|V|} \qquad \textbf{(5-2)}$$

5.2.3 Network Diameter (ϕ):

It is the measure of the maximum number of edges between any two nodes in the network. It is calculated using Eq. (5-3).

$$\phi = \max\left(N_E(v_i, v_j)\right) \forall\, v_i \in V, i \neq j \qquad \textbf{(5-3)}$$

where $N_E(v_i, v_j)$ is the minimum number of edges that need to be traversed between vertices v_i and v_j. It is an indicator of the topological spread and network efficiency of the water pipe network (Haegele 2016; Pandit and Crittenden 2012; Yazdani et al. 2011). Dijkstra's shortest path algorithm (Dijkstra 1959) was used to find the minimum number of edges needed to be traversed between any two vertices.

5.2.4 Average Geodesic Path Length ($\bar{L}$):

This metric estimates the average number of paths that need to be traversed to get from one node to other. It is calculated using Eq. (5-4)

$$\bar{L} = \frac{1}{|V|(|V|-1)} * \sum_{i \neq j} N_E(v_i, v_j) : \forall\ v_i \in V \qquad \textbf{(5-4)}$$

where $N_E(v_i, v_j)$ is the minimum number of edges that need to be traversed to reach from vertex v_i to v_j. Dijkstra's shortest path algorithm (Dijkstra 1959) was used to find the shortest path between the vertices. It provides an approximation of water pipe network's efficiency (Haegele 2016; Pandit and Crittenden 2012; Yazdani et al. 2011).

5.2.5 Transitivity or Global Clustering Coefficient (GCC):

It is defined by Wasserman and Faust (1994) as the fraction between the total number of triangles (N_Δ) and the total number of connected triples (N_3) as is shown by Eq. (5-5). It is a measure of the tendency of the nodes in the network to cluster or form triangles.

$$GCC = \frac{3N_\Delta}{N_3} \qquad \textbf{(5-5)}$$

It provides an estimate of the water pipe network's redundancy (Haegele 2016; Yazdani et al. 2011). The number of triangles in the network was found by calculating the trace of the adjacency matrix of the graph (i.e. the sum of main diagonal elements) while the number of triples was calculated by using a simple enumeration.

5.2.6 Meshedness Coefficient (MC):

As per Buhl et al. (2006), meshedness coefficient is defined as the fraction between the total and the maximum number of independent loops in a planar graph. It is calculated using Eq. (5-6).

$$MC = \frac{|E| - |V| + 1}{2|V| - 5} \qquad \textbf{(5-6)}$$

It provides an estimate of topological redundancy of water pipe network by calculating the ratio of the number of independent loops to the number of maximum loops (Haegele 2016; Paez and Filion 2017; Pandit and Crittenden 2012).

5.2.7 Central Point Dominance (CPD):

As per Freeman (1977), central point dominance is the average difference between the centrality of a node (C_i) to the centrality of most central node (C_{max}). It is calculated using Eq. (5-7).

$$CPD = \frac{1}{|V| - 1} \sum (C_{max} - C_i) \qquad \textbf{(5-7)}$$

where C_i is given by the ratio of the number of the shortest geodesic path between two vertices that pass-through node i to the total number geodesic path between the two vertices. It was calculated using the an algorithm proposed by Brandes (2001). This metric provides an estimate of robustness of the water pipe network (Pandit and Crittenden 2012; Yazdani et al. 2011).

5.2.8 Density of Articulation Points (ρ_{AP}):

Articulation point is a vertex in a graph such that its removal leads to isolation of a part of the graph. For water pipe networks, these points correspond to junctions whose damage leads to the isolation of a part of the water network. Density of articulation point is calculated using Eq. (5-8).

$$\rho_{AP} = \frac{N_{Ap}}{|V|} \qquad \textbf{(5-8)}$$

where N_{Ap} is the total number of articulation points in the graph. A simple depth first search (Cormen et al. 2009) was used to identify the articulation points in the graph. Large value of articulation point density indicates the presence of a large number of vulnerable points in the water pipe network. Hence, this metric is an estimate of robustness of water pipe networks (Paez and Filion 2017).

5.2.9 Density of Bridges (ρ_{Br}):

A bridge in a graph is a link such that its removal leads to the isolation of a part of the graph. For water pipe networks, these links correspond to pipes whose break leads to a part of the water pipe network being isolated. Density of bridges is calculated using Eq. (5-9).

$$\rho_{Br} = \frac{N_{Br}}{|E|.} \qquad (5-9)$$

where N_{Br} is the total number of bridges in the graph. A simple depth first search (Cormen et al. 2009) was used to identify the articulation points in the graph. High value of bridge density indicates the presence of a large number of vulnerable links in the network. Hence, this metric is an estimate of robustness of the water pipe networks (Paez and Filion 2017).

5.2.10 Spectral Gap (SG) (Estrada 2006):

It is the difference between first and second eigen values of the graph's adjacency matrix. For water pipe networks, it estimates the robustness and optimal connectivity layouts of the network (Yazdani et. al. 2011).

5.2.11 Algebraic Connectivity (AC) (Fiedler 1973):

This is the second smallest eigen value of the normalized Laplacian matrix of the network. For water pipe networks, it estimates the robustness and resistance of a network towards efforts to decouple the network (Pandit and Crittenden 2012; Yazdani et al. 2011).

5.3 Generating earthquake induced stochastic pipe damages and Monte Carlo simulation

The methodology of generating earthquake induced stochastic pipe damages and the Monte Carlo simulation is illustrated in the Figure 5-2.
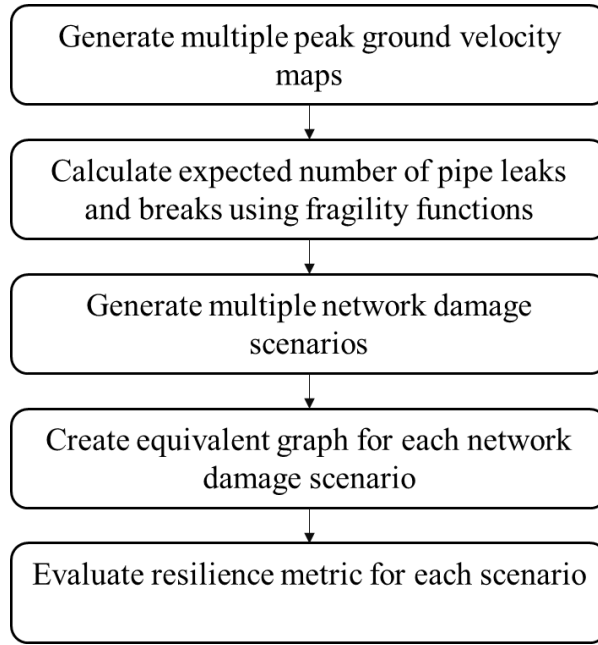
Figure 5-2. Simulation of stochastic seismic damages and Monte Carlo simulation

To initiate the analysis, expected seismic damages were evaluated. The methodology detailed in Pudasaini and Shahandashti (2018) was used for this. Accordingly, using seismic deaggregation analysis, an earthquake having maximum contribution ratio was identified (Adachi 2007). This earthquake was selected as the scenario earthquake. Using the magnitude and seismogenic characteristics of the scenario earthquake, the spatial distribution of Peak Ground Velocity (PGV) in the vicinity of water pipe network was mapped. To do this, the ground motion prediction model expressed by Eq. (5-10) was used.

$$log_{10}\left(PGV_{ij}\right) = f\left(M_i, \ R_{ij}, \ \boldsymbol{\theta_i}\right) + \sigma_B v_i + \sigma_W \boldsymbol{\epsilon_{ij}} \qquad \textbf{(5-10)}$$

where PGV_{ij} is the PGV for a site j due to the earthquake at source i, R_{ij} is the distance from the source i to site j, M_i is the magnitude of the earthquake event at source i, $\boldsymbol{\theta_i}$ are the seismogenic characteristics for the fault at source i, $\sigma_B v_i$ is the residual due to inter-event variability, and $\sigma_W \boldsymbol{\epsilon_{ij}}$ is the residual due to intra-event variability. A finite number of PGV maps were created to

accommodate the uncertainty of the spatial distribution of PGV caused by the simulated earthquake. Then, for each pipe for each PGV map, $PGVs$ were averaged along the pipe's length to get the average PGV for the pipe ($\overline{PGV_p}$).

After average PGV was determined for each pipe, its expected seismic repair rate was estimated using empirical fragility relationship given by ALA (2001). The formulation of expected seismic repair rate as per ALA (2001) is given by Eq. (6-11).

$$RR_p^m = K_p * 0.00187 * \overline{PGV}_p^m * (1 - x_p) \quad (6\text{-}11)$$

where RR_p^m is the expected seismic repair rate for pipe p and PGV map m (measured in number of damages per 304.8 m i.e. 1000 ft of pipe), K_p is the modification factor which considers the structural properties of pipe p (Tabulated in ALA (2001)), $\overline{PGV}_p^m$ is the average PGV for pipe p based on the PGV map m (measured in inches/second), x_p is the rehabilitation decision variable associated with pipe p which takes a value of 0 if the pipe is unrehabilitated and takes a value if 1 if the pipe is rehabilitated.

Using these expected seismic repair rate values, probabilistic leaks and breaks were simulated in the network using the Poisson process and leak probability matrix given by Shi (2006). Thousands of such damage scenarios were generated using Monte Carlo simulation. For each of these scenarios, an equivalent graph was created, and metrics described in the preceding section were calculated for the created graphs. The values of these metrics were then averaged over all the damage scenarios to estimate the expected value of those metrics for a rehabilitation decision. These expected values were then optimized.

5.4 Formulation of Stochastic Combinatorial Optimization

The optimization problem is formulated as a stochastic combinatorial optimization problem given by Eq. (5-12) and Eq. (5-13). The constraint represented by Eq. (5-13) is a knapsack constraint (Kellerer et al. 2004) imposed by the limited rehabilitation budget available to the water utilities.

$$max_{x \in X} E[y(x)] \qquad (5\text{-}12)$$

$$\sum_{p=1}^{\frac{|E|}{2}} a_p C_p \leq C_{max} \qquad (5\text{-}13)$$

where X is the set representing the decision space with every possible rehabilitation policy, $y(x)$ is a random variable representing the value of the metric measured for a damage scenario after the implementation of rehabilitation suggested by policy x, a_p is a binary variable to indicate rehabilitation decision based on policy x for pipe p, $\frac{|E|}{2}$ is half the number of edges in the graph i.e. total number of pipes in the network, C_p is the cost of proactive seismic rehabilitation for the pipe p. This is evaluated by cost estimation done using the latest cost data from RSMeans (2018), and C_{max} is the maximum rehabilitation budget.

The decision variable (x) is a vector. Each member of this vector (x_p) is associated with a pipe p in the water pipe network and the member's value indicates whether to rehabilitate or not to rehabilitate the pipe p. Hence, the decision space is a binary space and the problem is a combinatorial optimization problem. Furthermore, the problem is a stochastic optimization problem. This is due to the nature of the objective function. Here, random variable in the objective function $(y(x))$ is a stochastic quantity since the spatial distribution of PGV associated with the earthquake, the location of the pipe damages due to those velocities, and magnitude of such

damages are all stochastic. Therefore, the optimization problem is a stochastic combinatorial optimization.

5.5 Simulated Annealing Based Solution Methodology

Because of the combinatorial and stochastic nature of the objective function, simulated annealing based metaheuristic algorithm was used to solve the optimization problem. Simulated annealing based optimization is based on the process of physical annealing process in metals and was first proposed by Kirkpatrick et al. (1983). This is the earliest of all physics-based metaheuristic algorithms (Siddique and Adeli 2015). The configuration of atoms in solid annealing corresponds to the set of feasible solutions of simulated annealing; energy of atoms in solid annealing corresponds to the simulated annealing's objective function; and rate of decrease of temperature in solid annealing corresponds to the cooling schedule of simulated annealing (Siddique and Adeli 2016). Metropolis criterion proposed by Metropolis et al. (1953) is used by simulated annealing for accepting or rejecting the neighboring solution. Metropolis criterion used for simulated annealing when maximizing the objective function is given by the following steps.

Step 1: Find neighboring solution $x_n = N(x_i)$

Step 2: Calculate objective function at x_n i.e. $f(x_n)$

Step 3: If $f(x_n) < f(x_i)$, replace the old solution with new one i.e. $x_i = x_n$

Else if $[rand[0,1) < p(x_i, x_n)]$, replace the old solution with the new one i.e. $x_i = x_n$

Else keep the old solution.

Here, x represents the decision variable, x_n represents neighboring solutions,

$N(x)$ is the neighborhood function which gives neighboring solution by randomly disturbing the current solution,

$f(x)$ is the objective function evaluated at x,

$rand[0,1)$ is the uniformly distributed random number generator, and

$p(x_i, x_n)$ is the acceptance rule given by Boltzmann probability calculated using Eq. (5-14) where T is the current temperature.

$$p(x_i, x_n) = \exp(-\frac{f(x_i)-f(x_n)}{T}) \quad (5\text{-}14)$$

Simulated annealing is a trajectory based metaheuristic algorithm where only one solution is analyzed at a time and the direction of search for the next solution is given by the Boltzmann probability and metropolis criterion (Siddique and Adeli 2015). The behavior of simulated annealing is governed by the temperature (T). The algorithm starts at high temperature and decreases as the algorithm progress. The rate of decrease is dependent of the selection of cooling schedule adopted. At high temperature, the algorithm has high chance of selecting inferior solutions. This enables the algorithm to avoid getting stuck in local maximum. In contrast, at low temperature, the algorithm converges to the best available solution and tries to optimize it in its neighborhood. Selection of initial temperature, cooling schedule, and stopping criteria are highly dependent on the optimization problem at hand. Hence, these parameters usually fixed based on grid search to create the final solver (Chen and Shahandashti 2009).

Simulated annealing is a popular optimization algorithm and had shown good performance when used to solve optimization problems related to civil engineering (Chen and Shahandashti 2009; Hackl et al. 2018; Nayak and Turnquist 2016; Paya et al. 2008; Zeferino et al. 2009). One of the

strong attributes of metaheuristic-based optimizers such as simulated annealing is that they do not make any strong assumptions regarding the objective function such as its convexity or continuity. This makes them really powerful optimization tools when dealing with an objective function which does not have a closed form representation. Hence, to solve the optimization problem represented by Eq. (5-12) and Eq. (5-13) an optimization solver based on simulated annealing was created. Grid search was used to calibrate its maximum temperature, stopping criteria, and cooling schedule. The flow of simulated annealing designed to solve the optimization problem given by Eq. (5-12) and Eq. (5-13) is illustrated in Figure 5-3.
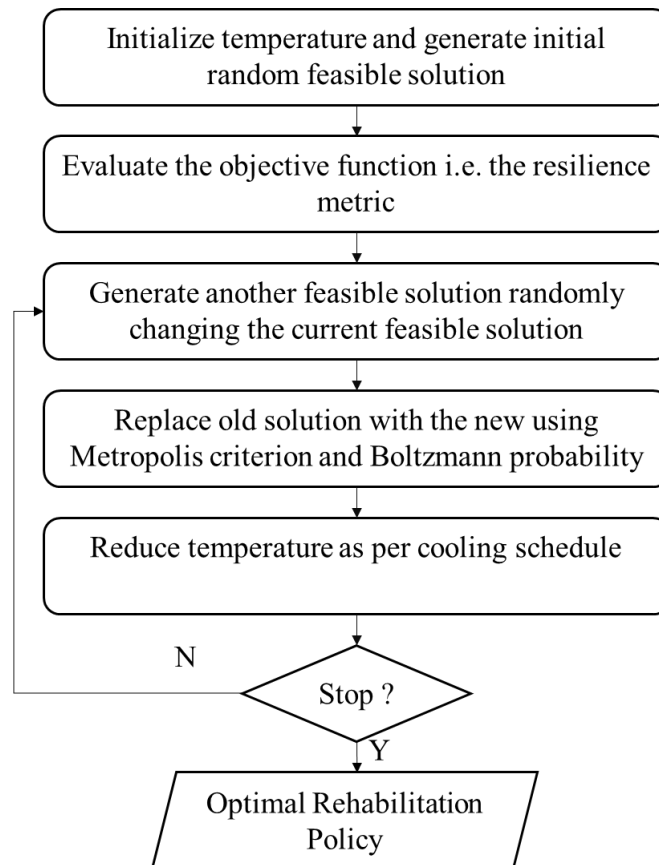

Figure 5-3. Flow of the simulated annealing

5.6 Evaluation of the performance of resilience metrics as the objective function

Optimization runtime was recorded for each simulated annealing run. Furthermore, the optimal policy identified by the simulated annealing using each resilience metric was evaluated using Eq. (5-14) and Eq. (5-15) to calculate the post-earthquake serviceability offered by the identified optimal policy. To calculate the left side of Eq. (5-14) and Eq. (5-15), the water pipe network was at first rehabilitated as per the suggestion of the respective rehabilitation policy. Then, the rehabilitated network was subjected to seismic ground motion intensities due to the selected scenario earthquake. After that, using Monte Carlo simulation described in preceding sections, thousands of damage scenarios were generated. These damage scenarios were then evaluated using quasi-static hydraulic analysis to calculate actual flows and pressure for each damage scenario. Available demand fraction (Ozger 2003), a measure of post-earthquake serviceability, was then calculated using Eq. (5-14) and Eq. (5-15).

$$y_n^j(x) = \begin{cases} 1, & P_n^j(x) \geq P_{min} \\ 0, & P_n^j(x) < P_{min} \end{cases} \qquad (5\text{-}15)$$

where $\overline{ADF(x)}$: Average available demand fraction for given rehabilitation policy x, $NMCS$: Maximum Monte Carlo Runs, $|V|$: Total number of nodes in the water pipe network i.e. the total number of vertices in the graph, Q_n : Water demand at node n, $y_n^j(x)$: Indicator function denoting if the demand is fulfilled t at node n or not for j^{th} Monte Carlo run for a given rehabilitation policy (x), $P_n^j(x)$: Hydraulic pressure at node n for j for j^{th} Monte Carlo run for a given rehabilitation policy (x), and P_{min} : Minimum pressure required to fulfill firefighting demand (0.14 MPa as per Trautman et al. (1987)).

Available demand fraction ($\overline{ADF(x)}$) and optimization runtime were then used to compare the optimal rehabilitation policies identified using different metrics as the objective function.

5.7 Results

A benchmark network (Centre for Water System 2017) simulating a city scale water pipe network was used for this study. The network consists of 317 pipes and 268 junctions. Four reservoirs act as the source of water for the network. The benchmark network is illustrated in Figure 5-4. Figure 5-5 shows the assumed arbitrary spatial distribution of pipes embedded in corrosive soil.
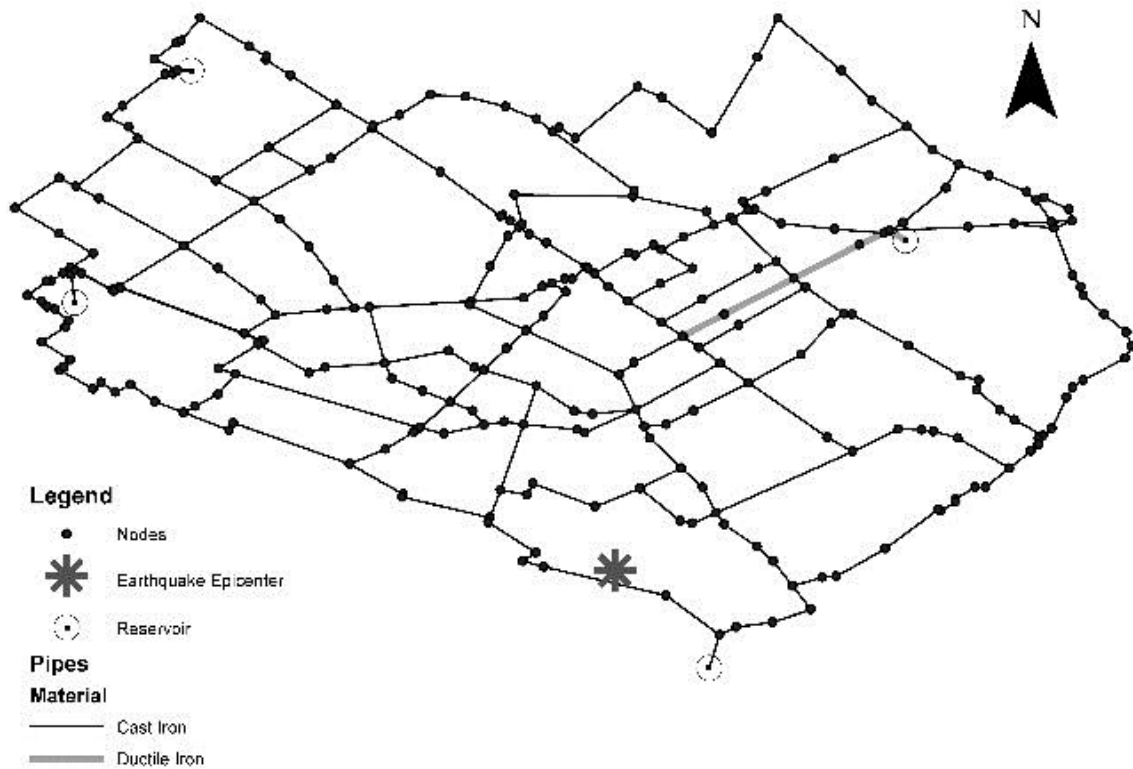
Figure 5-4. Benchmark network to illustrate the application of the proposed methodology

Legend

○   Junction

⊘   Reservoir

Pipes

—— 0 *In Non-Corrosive Soil*
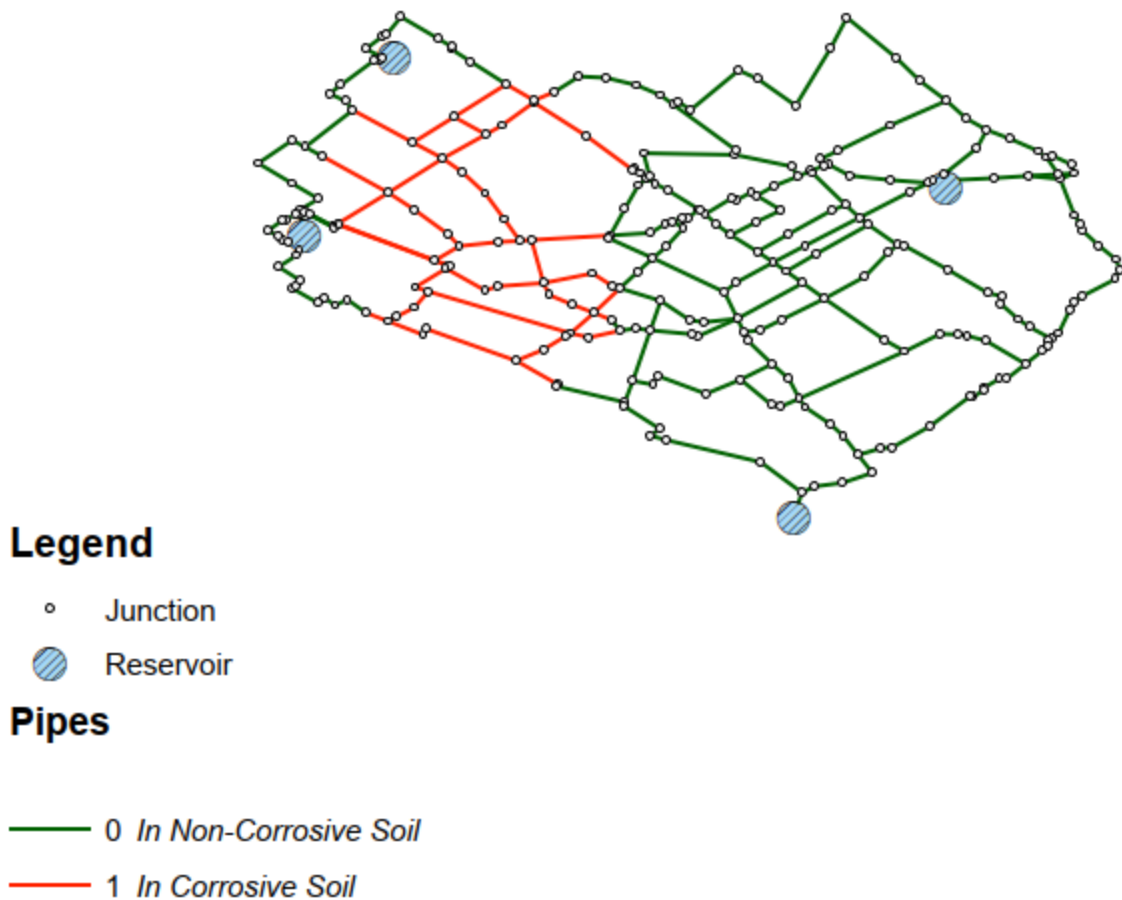
—— 1 *In Corrosive Soil*

Figure 5-5. Distribution of pipes embedded in corrosive soil

The rehabilitation cost constraint (C_{max}) was assumed to be 5 million US dollars. To have a spatial reference for seismic vulnerability analysis, this network was assumed to be in Pasadena, California. PGV maps were then generated for a scenario earthquake having an epicenter in the nearby Raymond fault. This scenario earthquake was selected based on a methodology involving seismic deaggregation analysis outlined in Adachi (2007). Figure 5-6 shows the spatial distribution of median peak ground velocity due to the scenario earthquake.
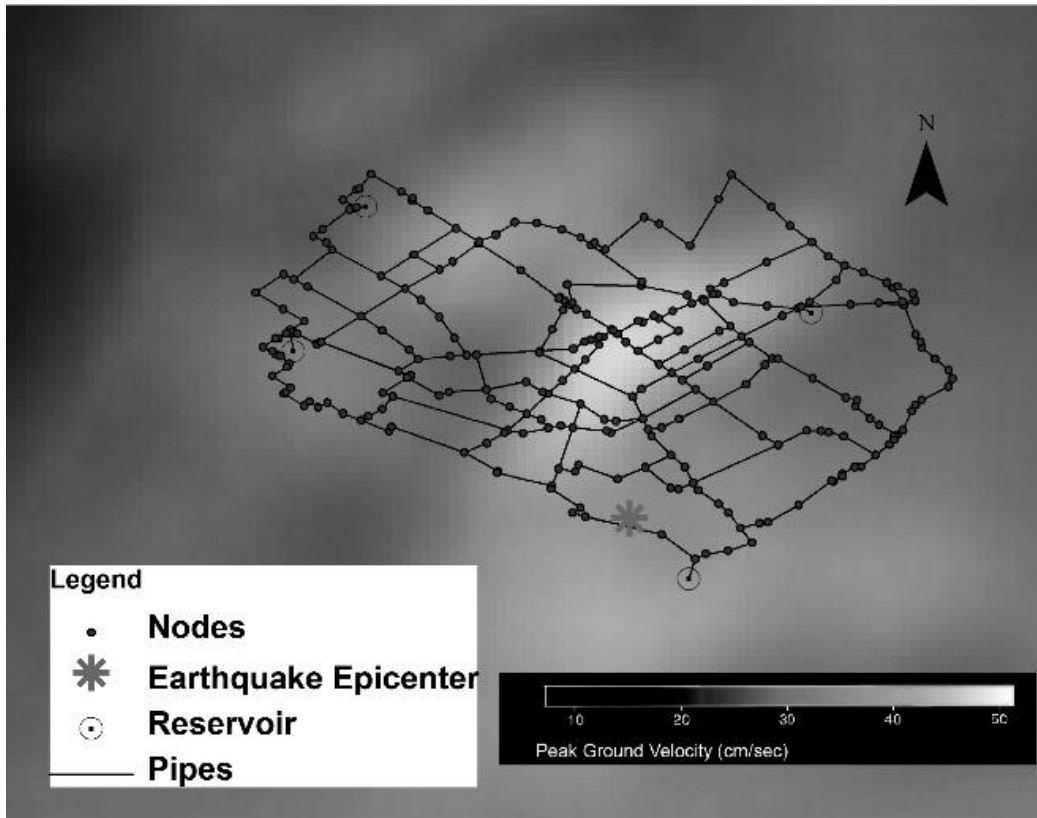
Figure 5-6. Spatial distribution of median peak ground velocity due to the scenario earthquake

Since different resilience metrics have different sensitivity to stochastic seismic damages, identification of sufficient Monte Carlo iterations for stabilizing the expected value for each metric was needed. Hence, before the optimization was started, a Monte Carlo convergence study was carried out to identify adequate Monte Carlo runs for each metric. Adequate Monte Carlo runs identified based on the convergence study for each metric is tabulated in Table 5-1. Table 5-1 also shows whether the metric was maximized or minimized. The decision to maximize and minimize was based on the calculation of a metric for the unrehabilitated network and completely rehabilitated network. For instance, average link density for the unrehabilitated network (for 900 Monte Carlo runs) was calculated as 0.00824 and for the completely rehabilitated network was calculated to be 0.00860. This shows that the metric should be maximized to enhance the resilience

of the network. This was done for each metric to identify the type of optimization needed to

enhance the resilience of the network. After identification of adequate Monte Carlo runs and the

type of optimization, an estimate of the runtime of simulated annealing was made. The parameters

of the simulated annealing used for this estimate are given in Table 5-2. The plot of the estimated

runtime for different metrics is shown in Figure 5-7.

Table 5-1. Adequate Monte Carlo runs identified based on convergence study

Metrics	Monte Carlo Runs	Optimization Type
Average Link Density	900	Maximization
Average Node Degree	900	Maximization
Meshedness Coefficient	900	Maximization
Articulation Point Density	2700	Minimization
Central Point Dominance	3700	Minimization
Available Demand Fraction	3000	Maximization

Table 5-2. Parameters of the final solver

Parameter	Value
Starting Temperature	100
Terminal Temperature	1
Cooling Schedule	Linear $(T_{i+1} = T_i - 2)$
Objective Evaluations at each Temperature	10
Maximum Monte Carlo Runs	Variable for each metric
Total Objective Evaluations	500

This estimation enabled the identification of the metrics which would have led to computationally prohibitive optimization runtime. For this study, an optimization runtime of 500 hours was adopted as the threshold value for computational feasibility in terms of runtime. Based on these criteria, average link density, average node degree, meshedness coefficient, articulation point density, central point dominance, and available demand fraction were selected for further analysis. Figure 5-7 also showed that even though hydraulic equations do not have to solved when evaluating topological metrics, evaluating some topological metrics might end up taking more time than hydraulic-based metrics such as available demand fraction due to the costly operations involved in calculating them.
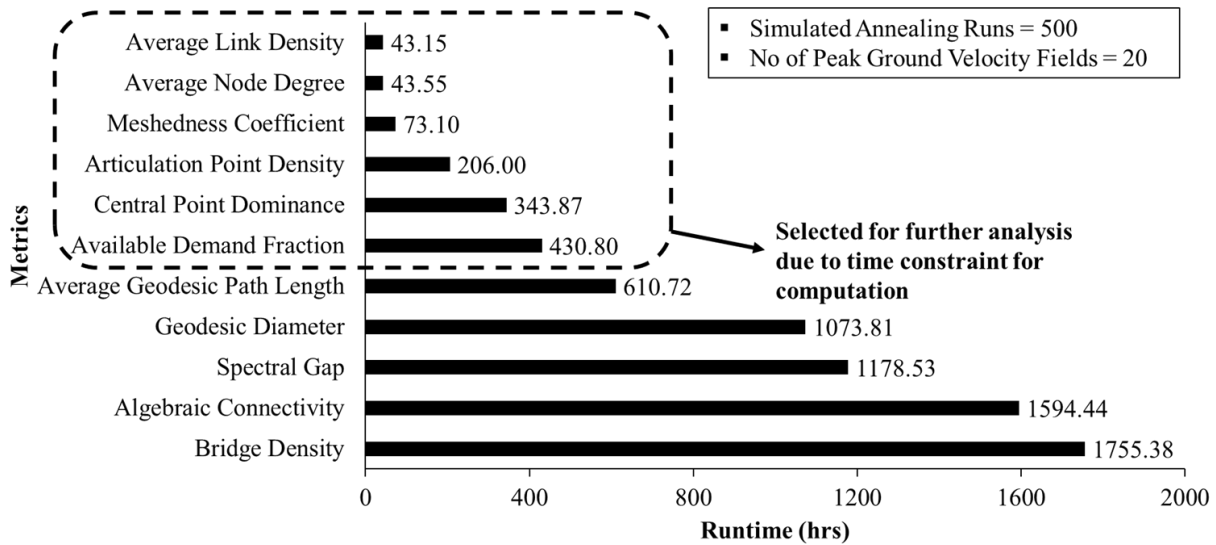
Figure 5-7. Runtime estimation for each metric

.Following the identification of metrics with feasible optimization runtime, these metrics were individually used as the objective in the simulated annealing to identify optimal rehabilitation

policies. The pipes recommended for rehabilitation by the optimal policies identified using each of these metrics are shown in Figure 5-8 with thick lines.
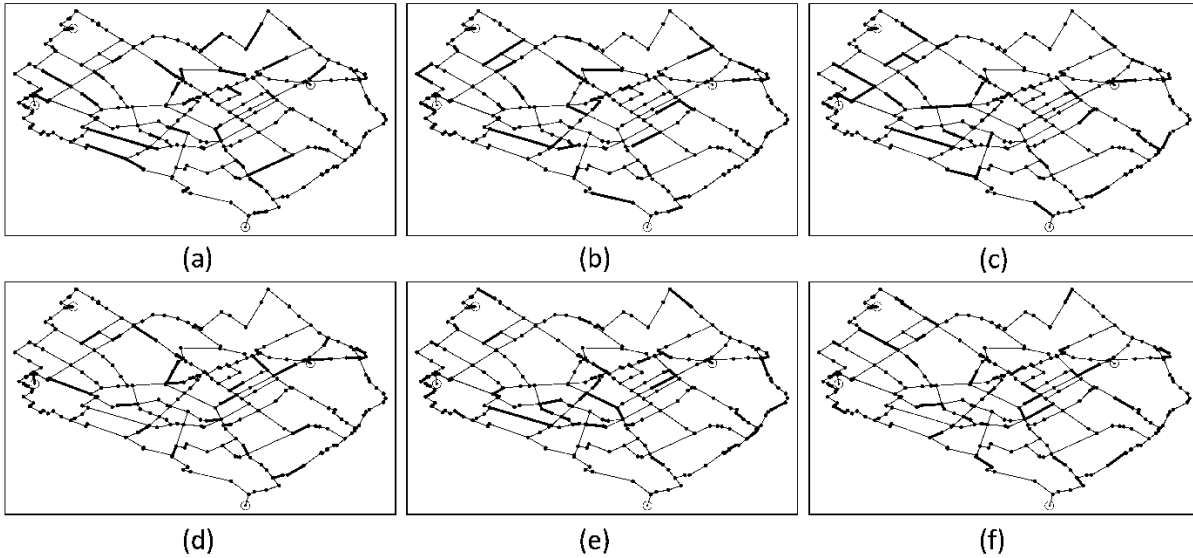
Figure 5-8. Optimal policies identified using objective based on (a) Average Link Density (b) Average Node Degree (c) Meshedness Coefficient (d) Articulation Point Density (e) Central Point Dominance (f) Available Demand Fraction

After the identification of these optimal policies, the post-earthquake performance of each of these policies was analyzed in terms of available demand fraction (Eq. (5-14)) which is the measure of post-earthquake serviceability offered by the rehabilitation policy. The results of such analyses are plotted in . Available demand fraction is plotted for optimal policy identified by using each of the six metric. Here, the confidence interval with 5 percent level of significance is also added to the plot of available demand fraction. As such, Figure 5-9 is a combined plot of available demand fraction and the optimization runtime for each resilience metric. The available demand fraction for the unrehabilitated case is also plotted in Figure 5-9 to illustrate that irrespective of the choice of metrics, significant improvement in post-earthquake serviceability was achieved. This figure

shows that metrics which have significantly low computational runtime (i.e. average link density and average node degree) yield rehabilitation policies which perform on par with the optimal policies identified by the use of metrics which have significantly high runtime (Central Point Dominance, Articulation Point Density, and Available Demand Fraction) in terms of post-earthquake serviceability. Here, despite much less optimization runtime, average link density-based optimization was able to yield a highly competent optimal policy. This policy had available demand fraction comparable to the available demand fraction of the optimal policy given by optimization which used available demand fraction itself as the objective function. This indicates that graph theory-based metrics such as average link density despite their low computational runtime may be used as a surrogate for hydraulics-based metrics such as available demand fraction to identify optimal rehabilitation policy for maximizing seismic resilience of water pipe network. This can be tremendously important for large urban pipe networks where a large number of pipes would lead to a large decision space making the use of hydraulic-simulation-based metrics such as available demand fraction for resilience optimization computationally prohibitive.
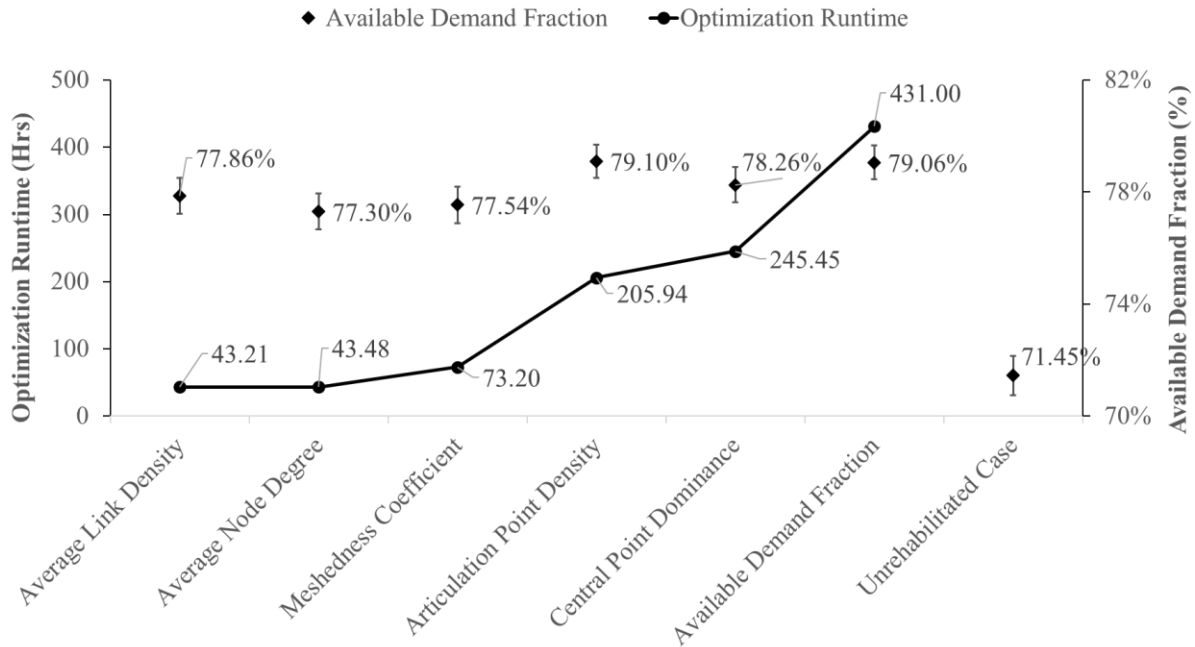
Figure 5-9. Comparison of optimal policies based on optimization runtime and post-earthquake

serviceability

5.8 Conclusions

A methodology has been proposed to study the performance of topological metrics when they are

used to formulate the objective functions to maximize the seismic resilience of the water pipe

networks.   The objective function to maximize the seismic resilience was formulated using

different graph theory-based topological metrics common in network analysis literature. The

resulting stochastic combinatorial optimization problem was then solved using a simulated

annealing-based optimization algorithm. For the optimization corresponding to each resilience

metric, the runtime of the optimization and post-earthquake serviceability of the optimal

rehabilitation policy was calculated. Comparison of these two quantities enabled the evaluation of

the metric's suitability for seismic optimization of large-scale water pipe networks. The results

obtained in this study showed that optimization using metrics which have significantly low

computational runtime (i.e. average link density and average node degree) can potentially yield rehabilitation policies which perform on par with the optimal policies identified by optimization using metrics which have significantly high runtime (Central Point Dominance, Articulation Point Density, and Available Demand Fraction) in terms of post-earthquake serviceability. Furthermore, the findings also demonstrated suitability of metrics having low computational time such as average link density as potential surrogates for computationally intensive hydraulic simulation-based resilience metrics such as available demand fraction for maximizing seismic resilience of water pipe networks.

These findings will be valuable for utility managers in charge of managing large water pipe networks where the use of typical hydraulic simulation-based metrics such as available demand fraction for optimization could be computationally prohibitive. For such cases, metrics such as average link density can be used as a surrogate for hydraulics-based metrics. This could result in optimization runtime reduction by several hours without any significant loss of solution quality.

CHAPTER 6

CONCLUSIONS

Although many researchers have proposed approaches for seismic vulnerability assessment for the water pipe networks, approaches to identify critical pipes for seismic rehabilitation of a water pipe network are rare. However, even these rare approaches are based on some simple prioritization techniques or ignore the correlation between the effect of pipes' damages on the network serviceability. As such, there was a need of an approach to identify critical pipes for pro-active seismic rehabilitation of water pipe networks that is based on comprehensive seismic vulnerability assessment; that considers spatial correlation between seismic intensities; that considers limited rehabilitation budget; and does not ignore the correlation between the effect of pipes' damages on the network serviceability. Furthermore, there is no literature that studies the performance of resilience metrics as the objective function for proactive seismic rehabilitation of water pipe network. Hence, this study was conducted, and based on the results, following conclusions were derived.

Task 1 Conclusions: An approach to identify critical pipes for resource-constrained seismic rehabilitation and to improve post-earthquake serviceability of a water pipe was created by integrating a genetic algorithm with a network-level seismic vulnerability assessment. This integration enables the identification of critical pipes, for distribution of rehabilitation resources at the system level. The application of the created approach was demonstrated using benchmark networks developed for testing algorithms dealing with formulating resilient designs of large water pipe networks. Furthermore, the results obtained from our proposed methodology was compared to the results obtained by using simple length prioritization scheme. Results demonstrated that the methodology created in this study outperforms the simple prioritization scheme practiced by

utilities. Additionally, the created approach was also validated by using identifying critical pipes for seismic rehabilitation in a water distribution network developed by the US EPA. These results were then compared with the latest methodology in literature. The comparison showed that our methodology identified more economical seismic rehabilitation policy compared to the most recent proposed approach in the literature when there are limitations about the length of pipes that can be rehabilitated. It is expected that the result of this study will help water utilities make informed decisions that will enhance post-earthquake serviceability of the water pipe networks.

Task 2 Conclusions: A simulated annealing-based optimization is developed and integrated with network-level seismic vulnerability assessment of water pipe network to maximize its post-earthquake serviceability by considering network-level distribution of limited rehabilitation resources. The developed approach is used to identify critical pipes for seismic rehabilitation of two benchmark networks. The results thus obtained were compared to the rehabilitation policy suggested by a simple length-based heuristic and the policy suggested by a latest methodology in literature. The comparison showed that our approach was able to identify more economical rehabilitation policy as compared to the simple length-based rehabilitation heuristic and the latest methodology in literature. The developed approach adds to the existing literature, a new method of considering network level distribution of limited rehabilitation resources for the seismic rehabilitation of water pipe networks. Moreover, the developed approach can be used by the water utility managers to formulate economical seismic rehabilitation policy for their water pipe networks when rehabilitation budget is constrained.

Task 3 Conclusions: Resource constrained seismic resilience optimization of water pipe networks using graph theory based metrics which have significantly low computational runtime (such as average link density and average node degree) can potentially yield rehabilitation policies which

perform on par with the optimal policies identified by the optimization with metrics which have significantly high runtime (Central Point Dominance, Articulation Point Density, and Available Demand Fraction) in terms of post-earthquake serviceability. Furthermore, the findings also demonstrated suitability of metrics having low computational time such as average link density as potential surrogates for computationally intensive hydraulic simulation-based resilience metrics such as available demand fraction for maximizing seismic resilience of water pipe networks.

These findings will be valuable for utility managers in charge of managing large water pipe networks where the use of typical hydraulic simulation-based metrics such as available demand fraction for optimization could be computationally prohibitive. For such cases, metrics such as average link density can be used as a surrogate for hydraulics-based metrics. This could result in optimization runtime reduction by several hours without any significant loss of solution quality.

REFERENCES

Abediniangerabi, B., Shahandashti, S. M., Bell, B., Chao, S.-H., and Makhmalbaf, A. (2018). "Building energy performance analysis of ultra-high-performance fiber-reinforced concrete (UHP-FRC) façade systems." *Energy and Buildings*, Elsevier B.V., 174, 262–275.

Abrahamson, N. A., and Silva, W. J. (2007). *Campbell-Bozorgnia NGA Ground Motion Relations for the Geometric Mean Horizontal Component of Peak and Spectral Ground Motion Parameters*. Berkeley.

Adachi, T. (2007). "Impact of Cascading Failures on Performance Assessment of Civil Infrastructure Systems." *Ph.D. Dissertation*, Georgia Institute of Technology.

Adachi, T., and Ellingwood, B. R. (2008). "Serviceability of earthquake-damaged water systems: Effects of electrical power availability and power backup systems on system vulnerability." *Reliability Engineering and System Safety*, 93(1), 78–88.

American Lifelines Alliance (ALA). (2001). *Seismic Fragility Formulations for Water Systems.*

Angeloudis, P., and Fisk, D. (2006). "Large subway systems as complex networks." *Physica A: Statistical Mechanics and its Applications*, 367, 553–558.

Apostolakis, G. E., and Lemon, D. M. (2005). "A Screening Methodology for the Identification and Ranking of Infrastructure Vulnerabilities Due to Terrorism." *Risk Analysis*, 25(2), 361–376.

Awumah, K., Goulter, I., and Bhatt, S. K. (1991). "Entropy-Based Redundancy Measures in Water-Distribution Networks." *Journal of Hydraulic Engineering*, 117(5), 595–614.

Ballantyne, D. B., and Taylor, C. (1990). "Earthquake loss estimation modeling of the Seattle

water system using a deterministic approach." *Lifeline Earthquake Engineering*, ASCE, New York, NY, 747--760.

Berche, B., Von Ferber, C., Holovatch, T., and Holovatch, Y. (2009). "Resilience of public transport networks against attacks." *European Physical Journal B*, 71(1), 125–137.

Bondy, J. A., and Murty, U. S. R. (2008). *Graduate Texts in Mathematics : Graph Theory. Springer*, Springer.

Bonneau, A. L., and O'Rourke, T. D. (2009). *Water supply performance during earthquakes and extreme events*. *Mceer*.

Brandes, U. (2001). "A faster algorithm for betweenness centrality." *Journal of Mathematical Sociology*, 25(2), 163–177.

Buhl, J., Gautrais, J., Reeves, N., Solé, R. V., Valverde, S., Kuntz, P., and Theraulaz, G. (2006). "Topological patterns in street networks of self-organized urban settlements." *The European Physical Journal B*, 49(4), 513–522.

Cavalieri, F., Franchin, P., Buriticá Cortés, J. A. M., and Tesfamariam, S. (2014). "Models for Seismic Vulnerability Analysis of Power Networks: Comparative Assessment." *Computer-Aided Civil and Infrastructure Engineering*, 29(8), 590–607.

Center of Water Systems. (2018). "Large Problems." <http://emps.exeter.ac.uk/engineering/research/cws/resources/benchmarks/design-resiliance-pareto-fronts/large-problems/> (Jan. 1, 2018).

Centre for Water System. (2017). "Benchmarks." <http://emps.exeter.ac.uk/engineering/research/cws/downloads/benchmarks/,> (May 1, 2017).

Chen, A., Yang, C., Kongsomsaksakul, S., and Lee, M. (2007). "Network-based acessibility measures for vulnerability analysis of degradable transportation networks." *Networks and Spatial Economics*, 7(3), 241–256.

Chen, P. H., and Shahandashti, S. M. (2007). "Modified Simulated Annealing Algorithm and Modified Two Stage Solution Finding Procedure for Optimizaing Linear Scheduling Projects with Multiple Resource Constraints." *Proceedings of the 24th International Symposium on Automation and Robotics in Construction, ISARC 2007*, Kochi, India.

Chen, P. H., and Shahandashti, S. M. (2009). "Hybrid of genetic algorithm and simulated annealing for multiple project scheduling with multiple resource constraints." *Automation in Construction*, Elsevier B.V., 18(4), 434–443.

Chen, P., and Shahandashti, S. M. (2008). "Stochastic scheduling with multiple resource constraints using a simulated annealing-based algorithm." *Proceedings of the 25th International Symposium on Automation and Robotics in Construction, ISARC 2008*, 447–451.

Cheung, P., J. E. Van Zyl, and Reis, R. L. F. (2005). "Extension of EPANET for pressure driven demand modeling in water distribution system." *Proceedings of international conference in Computer and Control in Water Industry*, University of Exeter, Exeter, UK, 203–208.

Cormen, T. H., Leiserson, C. E., L. Rivest, R., and Stein, C. (2009). "Introduction to Algorithms." The MIT Press, Cambridge, Massachusetts.

Crucitti, P., Latora, V., and Marchiori, M. (2005). "Locating Critical Lines in High-Voltage Electrical Power Grids." *Fluctuation and Noise Letters*, 05(02), L201–L208.

Cubrinovski, M., Bradley, B., Wotherspoon, L., Green, R., Bray, J., Wood, C., Pender, M., Allen,

J., Bradshaw, A., Rix, G., Taylor, M., Robinson, K., Henderson, D., Giorgini, S., Ma, K., Winkley, A., Zupan, J., O'Rourke, T., DePascale, G., and Wells, D. (2011). "Geotechnical aspects of the 22 February 2011 Christchurch earthquake." *Bulletin of the New Zealand Society for Earthquake Engineering*, 44(4), 205–226.

Cunha, M. da C., and Sousa, J. (1999). "Water Distribution Network Design Optimization: Simulated Annealing Approach." *Journal of Water Resources Planning and Management*, 125(4), 215–221.

Datta, T. K. (1999). "Seismic response of buried pipelines: a state-of-the-art review." *Nuclear Engineering and Design*, 192, 271–284.

Diestel, R. (2000). *Graph Theory*. Springer-Velarg.

Dijkstra, E. W. (1959). "A note on two problems in connexion with graphs." *Numerische Mathematik*, 1(1), 269–271.

Eusgeld, I., Kröger, W., Sansavini, G., Schläpfer, M., and Zio, E. (2009). "The role of network theory and object-oriented modeling within a framework for the vulnerability analysis of critical infrastructures." *Reliability Engineering and System Safety*, 94(5), 954–963.

FEMA - Federal Emergency Management Agency. (2013). *Hazus - MH 2.1 Technical Manual. Multi-hazard Loss Estimation Methodology, Earthquake Model*, Federal Emergency Management Agency, Washington, D.C.

Fiksel, J., Goodman, I., and Hecht, A. (2014). "Resilience: Navigating toward a Sustainable Future." *Solutions*, 5(September/October), 1–13.

Fisher, R. E., Bassett, G. W., Buehring, W. A., Collins, M. J., and Dickinson, D. C. (2010). *Constructing a Resilience Index for the Enhanced Critical Infrastructure Recovery Program.*

ANL/DIS-10-9, Chicago.

Fragiadakis, M., and Christodoulou, S. E. (2014). "Seismic reliability assessment of urban water networks." *Earthquake Engineering & Structural Dynamics*, Wiley Online Library, 43(3), 357–374.

Freeman, L. C. (1977). "A Set of Measures of Centrality Based on Betweenness." *Sociometry*, 40(1), 35.

Grigg, N. (2003). "Water Utility Security: Multiple Hazards and Multiple Barriers." *Journal of Infrastructure Systems*, 9(2), 81–88.

Gutiérrez-Pérez, J. A., Herrera, M., Pérez-García, R., and Ramos-Martínez, E. (2013). "Application of graph-spectral methods in the vulnerability assessment of water supply networks." *Mathematical and Computer Modelling*, Elsevier Ltd, 57(7–8), 1853–1859.

Hackl, J., Adey, B. T., and Lethanh, N. (2018). "Determination of Near-Optimal Restoration Programs for Transportation Networks Following Natural Hazard Events Using Simulated Annealing." *Computer-Aided Civil and Infrastructure Engineering*, 33(8), 618–637.

Haddaway, A. (2015). "Earthquake-Resitant Ductile Iron Pipe Makes U.S. Debut in Los Angeles." *WaterWorld*, <http://www.waterworld.com/articles/print/volume-31/issue-4/features/earthquake-resistant-ductile-iron-pipe-makes-u-s-debut-in-los-angeles.html> (May 7, 2017).

Haegele, T. M. (2016). "An Analysis of the City of Austin Pipe Networks Using Network and Information Theory." The University of Texas at Austin.

Haimes, Y. Y., Matalas, N. C., Lambert, J. H., Jackson, B. A., and Fellows, J. F. (1998). "Reducing Vulnerability of Water Supply Systems to Attack." *Journal of Infrastructure Systems*, 4(4),

164–177.

Han, Z. Y., and Weng, W. G. (2010). "An integrated quantitative risk analysis method for natural gas pipeline network." *Journal of Loss Prevention in the Process Industries*, Elsevier Ltd, 23(3), 428–436.

Holland, J. H. (1975). *Adaptation in natural and artificial systems: an introductory analysis with applications to biology, control, and artificial intelligence*. MIT press.

Honegger, D. G., and Eguchi, R. T. (1992). "Determination of the relative vulnerabilities to seismic damage for San Diego County Water Authority (SDCWA) water transmission pipelines." *October*, 1, 992.

Huang, F., Yang, Y., and He, L. (2007). "A flow-based network monitoring framework for wireless mesh networks." *IEEE Wireless Communications*, 14(5), 48–55.

Hwang, H., Chiu, Y. H., Chen, W. Y., and Shih, B. J. (2004). "Analysis of damage to steel gas pipelines caused by ground shaking effects during the Chi-Chi, Taiwan, Earthquake." *Earthquake Spectra*, 20(4), 1095–1110.

Hwang, H., Lin, H., and Shinozuka, M. (1998). "Seismic Performance Assessment of Water Delivery Systems." *Journal of Infrastructure Systems*, American Society of Civil Engineers, 4(3), 118–125.

Ingber, L. (1993). "Simulated annealing: Practice versus theory." *Mathematical and Computer Modelling*, 18(11), 29–57.

Jeon, S. S., and O'Rourke, T. D. (2005). "Northridge earthquake effects on pipelines and residential buildings." *Bulletin of the Seismological Society of America*, 95(1), 294–318.

JM Eagle. (2017). "PVC vs Ductile Iron Pipe Installed Cost Comparison Calculator."

<http://www.jmeagle.com/pvc-vs-ductile-iron-pipe-installed-cost-comparison-calculator>
(Jul. 7, 2017).

Juan, A. A., Faulin, J., Grasman, S. E., Rabe, M., and Figueira, G. (2015). "A review of simheuristics: Extending metaheuristics to deal with stochastic combinatorial optimization problems." *Operations Research Perspectives*, Elsevier Ltd, 2, 62–72.

Kashani, H., Ashuri, B., Lu, J., and Shahandashti, M. (2012). "A Real Options Model to Evaluate Investments in Photovoltaic (PV) Systems." *Construction Research Congress 2012*, American Society of Civil Engineers, Reston, VA, 1641–1650.

Kellerer, H., Pferschy, U., and Pisinger, D. (2004). *Knapsack Problems*. Springer Berlin Heidelberg, Berlin, Heidelberg.

Kirkpatrick, S., Gelatt, C. D., and Vecchi, M. P. (1983). "Optimization by Simulated Annealing." *Science*, 220(4598), 671–680.

Klise, K. A., Murray, R., and Walker, L. T. N. (2015). *Systems Measures of Water Distribution System Resilience*. Albuquerque, NM (United States).

Knight, B. (2017). "Mexico City Earthquake Reconnaissance – Day 3." *What's Happening*, <http://www.wrkengrs.com/mexico-city-earthquake-reconnaissance-day-4/> (Oct. 30, 2018).

Markov, I., O'Rourke, T. D., and Grigoriu, M. (1994). *An evaluation of seismic serviceability of water supply networks with application to the San Francisco auxiliary water supply system*. Buffalo, NY.

Maruyama, Y., Kimishima, K., and Yamazaki, F. (2011). "Damage Assessment of Buried Pipes Due To the 2007 Niigata Chuetsu-Oki Earthquake in Japan." *Journal of Earthquake and*

Tsunami, 05(01), 57–70.

Metropolis, N., Rosenbluth, A. W., Rosenbluth, M. N., Teller, A. H., and Teller, E. (1953). "Equation of State Calculations by Fast Computing Machines." *The Journal of Chemical Physics*, 21(6), 1087–1092.

Murray, R., Janke, R., and Uber, J. (2004). "The Threat Ensemble Vulnerability Assessment (TEVA) Program for Drinking Water Distribution System Security." *Critical Transitions in Water and Environmental Resources Management*, American Society of Civil Engineers, Reston, VA, 1–8.

Nayak, M. A., and Turnquist, M. A. (2016). "Optimal Recovery from Disruptions in Water Distribution Networks." *Computer-Aided Civil and Infrastructure Engineering*, 31(8), 566–579.

O'Rourke, M., and Ayala, G. (1993). "Pipeline damage due to wave propagation." *Journal of Geotechnical Engineering*, American Society of Civil Engineers, 119(9), 1490–1498.

Ouyang, M. (2014). "Review on modeling and simulation of interdependent critical infrastructure systems." *Reliability Engineering & System Safety*, Elsevier, 121, 43–60.

Ozger, S. S. (2003). "A semi-pressure-driven approach to reliability assessment of water distribution networks." Arizona State University.

Ozger, S. S., and Mays, L. W. (1994). "A Semi-Pressure-Driven Approach To Reliability Assessment of Water Distribution Networks." Arizona State University.

Paez, D., and Filion, Y. (2017). "Generation and Validation of Synthetic WDS Case Studies Using Graph Theory and Reliability Indexes." *Procedia Engineering*, The Author(s), 186, 143–151.

Pandey, P., Ahmed, A., Sapkota, A., Hossain, M. S., and Thian, B. (2019). "Performance

Evaluation of Pavement Subgrade by In Situ Moisture and Matric Suction Measurements." *Pavements : Geo-Congress 2019*, American Society of Civil Engineers, Reston, VA, 347–356.

Pandit, A., and Crittenden, J. C. (2012). "Index of network resilience (INR) for urban water distribution." *Critical Infrastructure Symposium*, (April 2012), 1–12.

Paya, I., Yepes, V., González-Vidosa, F., and Hospitaler, A. (2008). "Multiobjective optimization of concrete frames by simulated annealing." *Computer-Aided Civil and Infrastructure Engineering*, 23(8), 596–610.

Pineda-Porras, O., and Najafi, M. (2010). "Seismic Damage Estimation for Buried Pipelines: Challenges after Three Decades of Progress." *Journal of Pipeline Systems Engineering and Practice*, 1(1), 19–24.

Pudasaini, B., and Shahandashti, S. M. (2018). "Identification of Critical Pipes for Proactive Resource-Constrained Seismic Rehabilitation of Water Pipe Networks." *Journal of Infrastructure Systems*, 24(4), 04018024.

Pudasaini, B., Shahandashti, S. M., and Razavi, M. (2017). "Identifying Critical Links in Water Supply Systems Subject to Various Earthquakes to Support Inspection and Renewal Decision Making." *Computing in Civil Engineering 2017*, American Society of Civil Engineers, Reston, VA, 231–238.

Reed, D. A., Kapur, K. C., and Christie, R. D. (2009). "Methodology for assessing the resilience of networked infrastructure." *IEEE Systems Journal*, 3(2), 174–180.

Rokneddin, K., Sánchez-Silva, M., and Dueñas-Osorio, L. (2009). "Reduced Computational Complexity for the Reliability Assessment of Typical Infrastructure Topologies." *TCLEE*

2009, American Society of Civil Engineers, Reston, VA, 1–12.

RSMeans. (2018). *2018 Heavy Construction Costs Book*. RSMeans Co, Rockland, MA.

Sapkota, A., Ahmed, A., Pandey, P., Hossain, M. S., and Lozano, N. (2019a). "Stabilization of Rainfall-Induced Slope Failure and Pavement Distresses Using Recycled Plastic Pins and Modified Moisture Barrier." *Landslides : Geo-Congress 2019*, American Society of Civil Engineers, Reston, VA, 237–246.

Sapkota, A., Hossain, S., Ahmed, A., and Pandey, P. (2019b). "Effect of Modified Moisture Barrier on the Slope Stabilized with Recycled Plastic Pins." *98th Annual Meeting of Transportation Research Board*, Transportation Research Board, Washington, D.C.

Selina, L., Davidson, R., Ohnishi, N., and Scawthorn, C. (2008). "Fire Following Earthquake-Reviewing the State-of-the-Art of Modeling." *Earthquake Spectra*, Earthquake Engineering Research Institute, 24(4).

Shahandashti, S. M., Abediniangerabi, B., Bell, B., and Chao, S. H. (2017). "Probabilistic Building Energy Performance Analysis of Ultra-High-Performance Fiber-Reinforced Concrete (UHP-FRC) Façade System." *Computing in Civil Engineering 2017*, American Society of Civil Engineers, Reston, VA, 223–230.

Shahandashti, S. M., and Pudasaini, B. (2019). "Proactive Seismic Rehabilitation Decision-Making for Water Pipe Networks Using Simulated Annealing." *Natural Hazards Review*, 20(2), 04019003.

Shahandashti, S. M., Razavi, S. N., Soibelman, L., Berges, M., Caldas, C. H., Brilakis, I., Teizer, J., Vela, P. A., Haas, C., Garrett, J., Akinci, B., and Zhu, Z. (2010). "Data-Fusion Approaches and Applications for Construction Engineering." *Journal of Construction Engineering and*

Management, 137(10), 863–869.

Shi, P. (2006). "Seismic response modeling of water supply systems." Cornell University.

Shuang, Q., Zhang, M., and Yuan, Y. (2014). "Node vulnerability of water distribution networks under cascading failures." *Reliability Engineering & System Safety*, Elsevier, 124, 132–141.

Siddique, N., and Adeli, H. (2015). "Nature Inspired Computing: An Overview and Some Future Directions." *Cognitive Computation*, Springer US, 7(6), 706–714.

Siddique, N., and Adeli, H. (2016). "Simulated Annealing, Its Variants and Engineering Applications." *International Journal on Artificial Intelligence Tools*, 25(06), 1630001.

Southern California Earthquake Data Center (SCEDC). (2018). "Significant Earthquakes and Faults." <http://scedc.caltech.edu/significant/raymond.html> (Mar. 1, 2018).

Sullivan, J. L., Novak, D. C., Aultman-Hall, L., and Scott, D. M. (2010). "Identifying critical road segments and measuring system-wide robustness in transportation networks with isolating links: A link-based capacity-reduction approach." *Transportation Research Part A: Policy and Practice*, Elsevier Ltd, 44(5), 323–336.

Thapa, B. R., Ishidaira, H., Pandey, V. P., and Shakya, N. M. (2016). "Impact Assessment of Gorkha Earthquake 2015 on Portable Water Supply in Kathmandu Valley: Preliminary Analysis." *Journal of Japan Society of Civil Engineers, Ser. B1 (Hydraulic Engineering)*, 72(4), I_61-I_66.

Trautman, C. H., Khater, M. M., O'Rourke, T. D., and Grigoriu, M. D. (1987). "Modeling water supply systems for earthquake response analysis." *Development in Geotechnical Engineering Vol 45., Structures and Stochastic Methods*, A. S. Cakmak, ed., Elsevier Science Publishing Company, New York, N.Y., 215–236.

United States Environmental Protection Agency (US EPA). (2002). "The Clean Water and Drinking Water Infrastructure Gap Analysis." 54.

United States Geological Survey (USGS). (2018a). "Unified Hazard Tool." *Earthquake Hazards Program*, <https://earthquake.usgs.gov/hazards/interactive/> (Mar. 1, 2018).

United States Geological Survey (USGS). (2018b). "U.S. Quaternary Faults and Folds Database." <https://usgs.maps.arcgis.com/apps/webappviewer/index.html?id=5a6038b3a1684561a9b0a adf88412fcf> (Jan. 1, 2018).

Wang, M., and Takada, T. (2005). "Macrospatial correlation model of seismic ground motions." *Earthquake Spectra*, 21(4), 1137–1156.

Wang, Y., Au, S.-K., and Fu, Q. (2010). "Seismic risk assessment and mitigation of water supply systems." *Earthquake Spectra*, Earthquake Engineering Research Institute, 26(1), 257–274.

Wasserman, S., and Faust, K. (1994). *Social Network Analysis : Methods and Applications*. Cambridge University Press, New York, NY.

Weatherill, G., Silva, V., Crowley, H., and Bazzurro, P. (2013). "Exploring Strategies for Portfolio Analysis in Probabilistic Seismic Loss Estimation." *Vienna Congress on Recent Advances in Earthquake Engineering and Structural Dynamics*, Vienna University of Technology, Vienna, Austria, 28–30.

Wolsey, L. A., and Nemhauser, G. L. (1999). *Integer and Combinatorial Optimization*. John Wiley & Sons, Inc.,.

Yasuda, S., Harada, K., Ishikawa, K., and Kanemaru, Y. (2012). "Characteristics of liquefaction in Tokyo Bay area by the 2011 Great East Japan Earthquake." *Soils and Foundations*, Elsevier, 52(5), 793–810.

Yazdani, A., and Jeffrey, P. (2011). "Robustness and Vulnerability Analysis of Water Distribution Networks Using Graph Theoretic and Complex Network Principles." *Water Distribution Systems Analysis 2010*, American Society of Civil Engineers, 933–945.

Yazdani, A., Otoo, R. A., and Jeffrey, P. (2011). "Resilience enhancing expansion strategies for water distribution systems: A network theory approach." *Environmental Modelling and Software*, Elsevier Ltd, 26(12), 1574–1582.

Yerri, S. R., Piratla, K. R., Matthews, J. C., Yazdekhasti, S., Cho, J., and Koo, D. (2017). "Empirical analysis of large diameter water main break consequences." *Resources, Conservation and Recycling*, 123, 242–248.

Zahed, S. E., Mohsen Shahandasht, S., and Najafi, M. (2017). "Investment Valuation of an Underground Freight Transportation (UFT) System in Texas." *Pipelines 2017*, American Society of Civil Engineers, Reston, VA, 192–201.

Zanini, M. A., Faleschini, F., and Pellegrino, C. (2017). "Probabilistic seismic risk forecasting of aging bridge networks." *Engineering Structures*, Elsevier Ltd, 136, 219–232.

Zanini, M. A., Vianello, C., Faleschini, F., Hofer, L., and Maschio, G. (2016). "A framework for probabilistic seismic risk assessment of NG distribution networks." *Chemical Engineering Transactions*, 53, 163–168.

Zeferino, J. A., Antunes, A. P., and Cunha, M. C. (2009). "An efficient simulated annealing algorithm for regional wastewater system planning." *Computer-Aided Civil and Infrastructure Engineering*, 24(5), 359–370.

Zohra, H. F., Mahmouda, B., and Luc, D. (2012). "Vulnerability assessment of water supply network." *Energy Procedia*, 18, 772–783.

Zolfaghari, M. R., and Niari, M. A. (2009). "Probabilistic Seismic Damage Assessment for Water Supply Networks following Earthquake." *TCLEE 2009*, American Society of Civil Engineers, Reston, VA, 1–11.